

Santa Clara University

Scholar Commons

Electrical and Computer Engineering Senior
Theses

Engineering Senior Theses

Spring 2022

Cost Efficient Radio Telescope

Nick Arroyo

Brian Benedicto

Tyler Ikehara

Follow this and additional works at: https://scholarcommons.scu.edu/elec_senior



Part of the [Electrical and Computer Engineering Commons](#)

SANTA CLARA UNIVERSITY

Department of Electrical and Computer Engineering

I HEREBY RECOMMEND THAT THE THESIS PREPARED
UNDER MY SUPERVISION BY


Nick Arroyo, Brian Benedicto, and Tyler Ikehara

ENTITLED

COST EFFICIENT RADIO TELESCOPE

BE ACCEPTED IN PARTIAL FULFILLMENT OF THE REQUIREMENTS
FOR THE DEGREE OF

BACHELOR OF SCIENCE
IN
ELECTRICAL ENGINEERING
AND IN
ELECTRICAL AND COMPUTER ENGINEERING



Thesis Advisor(s) (use separate line for each advisor)

June 4, 2022

date



Department Chair(s) (use separate line for each chair)

June 7th, 2022

date

COST EFFICIENT RADIO TELESCOPE

By

Nick Arroyo, Brian Benedicto, and Tyler Ikehara

SENIOR DESIGN PROJECT REPORT

Submitted to
the Department of Electrical and Computer Engineering

of

SANTA CLARA UNIVERSITY

in Partial Fulfillment of the Requirements
for the degree of Bachelor of Science
in Electrical Engineering and in Electrical and Computer Engineering

Santa Clara, California

Spring 2022

Abstract

This project aims to construct a smaller and less expensive radio telescope compared to traditional radio telescope designs by utilizing a Software Defined Radio (SDR). This is the first stage of a multi-year effort to bring radio astronomy capabilities to Santa Clara University. The implementation of this project includes designing and building a pyramidal horn antenna centered around the hydrogen line frequency of 1420 MHz. The project will also be comparing specifications of low noise amplifiers (LNA) and designing band-pass filters. Lastly, this project implements an SDR to process the signals received by the telescope to recreate a map of the movements of celestial objects in the galaxy.

Acknowledgements

We would like to thank our advisors, Dr. Kurt Schab and Dr. Shoba Krishnan, for all of their support and advice over the span of this project. We would also like to thank the Santa Clara University School of Engineering and Xilinx for providing us with funding grants that made it possible for to purchase the equipment needed to complete the project.

Contents

1	Introduction	1
1.1	Problems, Objectives, and Motivations	1
1.2	Background Information	1
1.3	Project Plan	2
1.4	Alternative Implementation Solutions	4
1.5	Ethical Considerations	5
1.6	Professional Issues and Constraints	5
2	Project Design	6
2.1	Antenna and Waveguide	6
2.1.1	Antenna Design Specifications	6
2.1.2	HFSS Simulations	11
2.1.3	Horn Antenna Construction	12
2.2	Filters	17
2.2.1	Filtering Topologies	17
2.2.2	Coupled Line Filter Design	17
2.2.3	Lumped Element Filter Design	19
2.3	Software Defined Radio and Data Processing	20
2.3.1	GNU Radio Installation	20
2.3.2	Recording Packets and Plot Generation	21
3	Project Outcomes	23
3.1	Antenna and Waveguide	23
3.1.1	Impedance Match Verification	23
3.1.2	Antenna Directivity Verification	26
3.2	Filters and Amplifiers	29
3.2.1	Filter Implementation	29
3.2.2	Coupled Line Filter Robustness	29

3.2.3	Amplifier Gain Tests	30
3.3	Software Defined Radio and Data Processing	32
3.4	Full System Trials	37
4	Conclusion	42
4.1	Final Design Assessment	42
4.2	Concluding Thoughts and Future Work	42
A	Appendix	44
A.1	Equipment List	44
A.2	Senior Design Conference Slides	46

List of Figures

1	Project block diagram. Adapted from [1].	2
2	Gantt Chart outlining the quarterly schedule for each module of the overall project.	3
3	a. Overall geometry of pyramid horn antenna; b. E-field plane dimensions; c. H-field plane dimensions. Adapted from [2].	7
4	Horn dimensions A and B vs Gain.	9
5	Secondary horn dimensions from Fig. 3b and 3c vs. Gain.	10
6	HFSS model of designed horn antenna with annotated dimensions. . .	11
7	Simulated gain of HFSS model. Red lobes are the main lobes pointing in the direction of the opening of the horn.	12
8	Constructed pyramidal horn section.	14
9	Waveguide probe connection.	15
10	Constructed waveguide section.	15
11	Completely constructed pyramidal horn antenna.	16
12	Coupled line filter layout	19
13	Lumped element bandpass filter. Adapted from [3].	20
14	Horn antenna connected to Fieldfox Network Analyzer for impedance test.	24
15	S_{11} vs. Frequency of constructed horn antenna.	25
16	Directivity test set up, tape markings denote different angle measurement placement.	27
17	Normalized power vs. Azimuth angle for HFSS simulation and the over-the-air experiment.	28
18	4 th & 7 th order coupled line filter performance histogram	30
19	Amplifier Gain Comparison	31
20	RF Test Signal Setup	34
21	RTL-SDR Blog V3 Waterfall Plot and Spectrum Analysis.	35

22	Ettus B210 Waterfall Plot and Spectrum Analysis.	36
23	Full System Setup	38
24	Recording modulated 1420MHz test signal over the air every second.	39
25	Recording the same modulated 1420MHz test signal over the air every 5 seconds.	39
26	Antenna pointing to empty space.	40
27	Antenna pointing to the Sun.	41

List of Tables

1	Initial pyramidal horn antenna design dimensions.	10
2	Equipment list and overall budget for the project.	45

1 Introduction

1.1 Problems, Objectives, and Motivations

Radio astronomy is a powerful way for researchers to study the positions and movements of objects in the universe. However, most radio telescopes are large in size and require expensive hardware and software. These factors make radio astronomy an elusive field of study for less experienced scientists, engineers and hobbyists. With this in mind, the objective of this project is to design a more cost-efficient and accessible radio telescope.

1.2 Background Information

The backbone of radio astronomy is the radio frequency emissions of hydrogen atoms surrounding celestial bodies. As the electrons in these clouds are excited between their fundamental states, they release electromagnetic energy with a frequency of $f_c = 1420$ MHz. As we know the frequencies at which these objects will radiate, it is possible to design antenna systems that can receive these signals. These systems are known as radio telescopes and they are essentially large directional antennas that operate at a very specific band of frequencies.

Radio telescopes are often extremely large and require expensive project sites due to the precise equipment required to receive the low power astronomical electromagnetic signals. In general, these telescopes are comprised of a large antenna, a series of filters and LNAs, and rather complex data processing hardware. This complexity makes it unreasonable to use one of these systems in an amateur setup. A solution for this problem is to replace most of the hardware in radio telescopes with a single Software Defined Radio (SDR).

SDRs are unique in the fact that the user can change its function through software instead of hardware. That is also the main limitation for SDRs, as the amalgamation

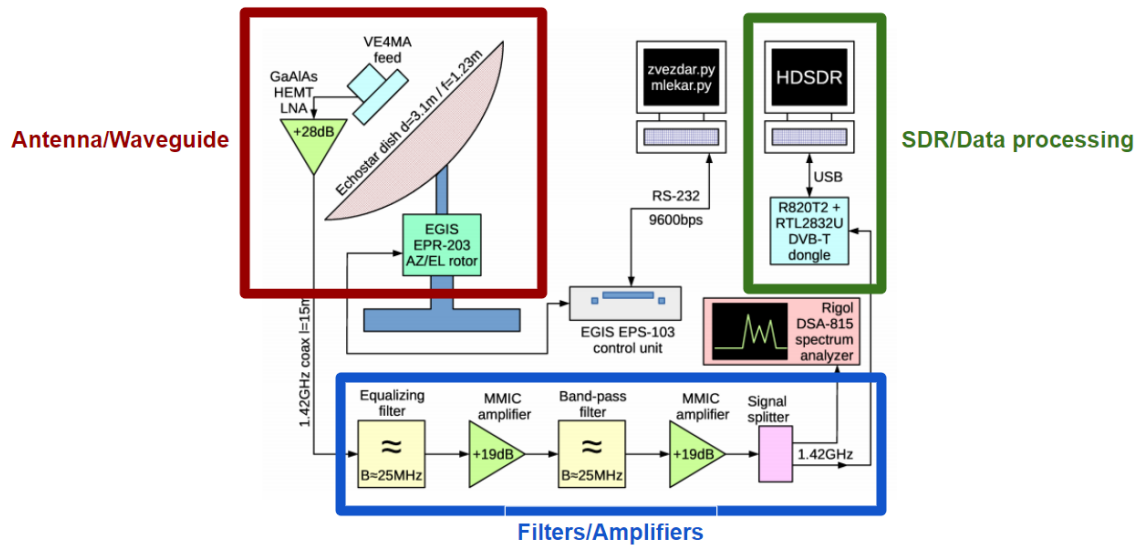


Figure 1: Project block diagram. Adapted from [1].

of software and hardware engineering typically increases the amount of personnel and complexity in a project. The ability to change the radio through software is especially useful as we can emulate the behavior of the complex hardware found in traditional radio telescopes by reprogramming a SDR. Additionally, there are also many open-source software programs such as GNU Radio that are able to reprogram most SDRs. Most importantly, SDRs are relatively inexpensive and easy to purchase.

1.3 Project Plan

To best quantify our project progress we have split our milestones into three separate categories. These categories are the main components to our project which include the antenna/waveguide design, filters and amplifiers, and software/data processing. A comprehensive configuration of these components is shown in Figure 1. This is a block diagram modified from a similar project that we will use for reference for this project[1].

The plan for this project is shown in detail with the Gantt chart in Figure 2. By splitting the project itself as well as its progress using these three section we are

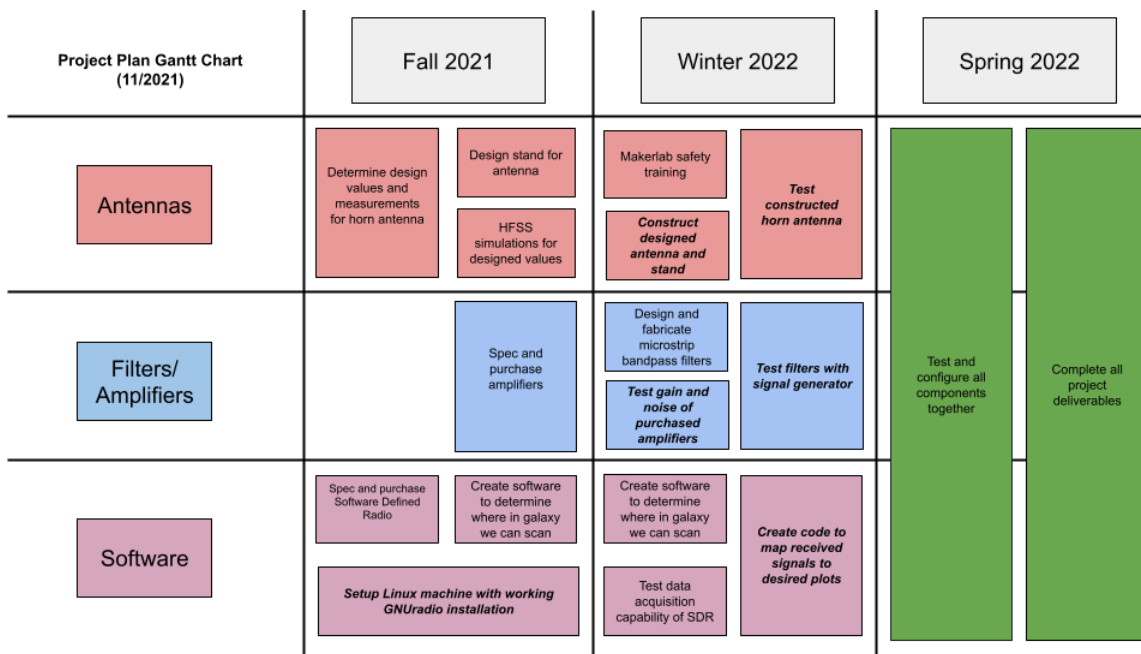


Figure 2: Gantt Chart outlining the quarterly schedule for each module of the overall project.

able to more narrowly focus in on each individual milestone of our project making objectives more understandable as well as attainable. The chart is further split into fall, winter, and spring quarters respectively.

The fall quarter objectives for antenna design included calculating design dimensions for the pyramidal horn antenna, designing the stand for the antenna, as well as simulating the pyramidal horn antenna in Ansys High-Frequency Structure Simulator (HFSS). The objectives for the amplifiers and filters included choosing specifications for these components and finalizing these purchases. On the software side, our project plans were to choose the SDR specifications and finish SDR purchasing, create software that determines the observable bodies from our position on earth, and finally to set up a Linux machine with a functioning and compatible version of GNU Radio.

The winter quarter objectives for the antenna design included receiving Maker Lab safety and tools training, constructing the pyramidal horn antenna, and testing the pyramidal horn antenna. On the filters and amplifiers side we aimed to design and

fabricate microstrip bandpass filters, test gain and noise of purchased amplifiers, and test the fabricated filters with the bench test equipment provided in the RF laboratory. For the software aspect we planned to continue with the observable bodies locating software, test the acquisition capabilities of the SDR, and create code to map received signals to desired plots.

Finally, for the spring quarter the main objective was to have all technical applications of our project completed and the entire radio telescope configured and acquiring data by the end of the first half of the quarter. This gave ample time to debug and verify that each module could work together.

1.4 Alternative Implementation Solutions

As our project is modular in nature, it was important that we have alternative back-up plans in case one of the modules does not function as intended.

For the antenna system, it was decided to use a pyramidal horn antenna to capture and focus electromagnetic radiation. This type of antenna was chosen due to its simplicity of design and construction as well as its capabilities. Another possible implementation would be a parabolic dish antenna. However, this design would be much more difficult to fabricate due to the parabolic shape which is much harder to construct. Furthermore, this implementation could be purchased, but would drastically, and unnecessarily, increase our budget.

For the amplifiers and filters section of the project, multiple amplifiers with varying noise figures and gain were purchased. By having multiple amplifiers we can not only have alternatives but also multiple datasets that compare price and effectiveness. A microstrip bandpass filter was also designed to be used in the filtering system. The alternative to this filter was a lumped component bandpass filter which include capacitors and inductors.

The signal processing portion of this project had fewer alternatives that are in the

scope of our implementations. However, the project considered two different types of SDRs that were tested and compared for implementation. One was a more inexpensive hobbyist level SDR while the other was a commercial grade SDR.

1.5 Ethical Considerations

One of the main ethical concerns that this project addresses is giving more people access to STEM learning experiences. By designing a cost efficient radio telescope, we can create opportunities for citizen science. Citizen science is research conducted, either in part or in whole, by amateur scientists. By making the tools of research more accessible, you can create a network of data acquisition around the globe. Radio astronomy is particularly dependent on antenna arrays, which widen the field of view of a project site. By giving more citizens radio telescope capabilities, you can theoretically expand the field of view of radio astronomy thanks to amateur scientists. More importantly, it can give young scientists and hobbyists easier and earlier access to technology and experiments that they can learn from.

1.6 Professional Issues and Constraints

As the project is concerned with receiving radio signals, it is vital that it follows the constraints set by the FCC, otherwise it could potentially harm or inhibit other important Radio Frequency operations. The main FCC constraint that the project needs to follow is to operate only within the allotted frequency band for radio astronomy, between 1400 MHz and 1427 MHz. It is also important that the system does not transmit signals above a certain power threshold. For this point, the project is designed to be a receive only system, so this constraint should not be an issue.

2 Project Design

2.1 Antenna and Waveguide

As the signals received in radio astronomy are extremely low in power, radio telescopes need to have directive antennas with high gain. Traditional radio telescope systems typically achieve this through the use of large parabolic dish antennas. However, for amateur radio astronomers, these type of antennas are costly and difficult to construct.

An alternative antenna design that amateur radio astronomers typically choose are pyramidal horn antennas as they are much easier to construct. Pyramidal horn antennas also have extra shielding due to its geometry, which reduces the side-lobes in its radiation pattern. This is beneficial as it reduces the amount of noise that the antenna receives from its surrounding environment.

The reason why this topology is not typically used in large radio astronomy projects is because its gain to size ratio is much lower than parabolic dish antennas. However, it is important to note that for the sake of this project, the desired gain is low enough that the size of the antenna will not be a limiting factor. With all of these considerations in mind, this project will implement a pyramidal horn antenna.

The geometry of the pyramidal horn antenna that this project will use can be seen in Fig. 3

2.1.1 Antenna Design Specifications

In order to calculate the initial design specifications, the rectangular waveguide dimensions a and b needed to be selected. These waveguide dimensions are typically set to a universal standard that is specific for certain frequency ranges. For the design center frequency, $f = 1420$ MHz, the Electronics Industries Alliance standard waveguide is the WR650 with $a = 165.1$ mm and $b = 82.55$ mm [4].

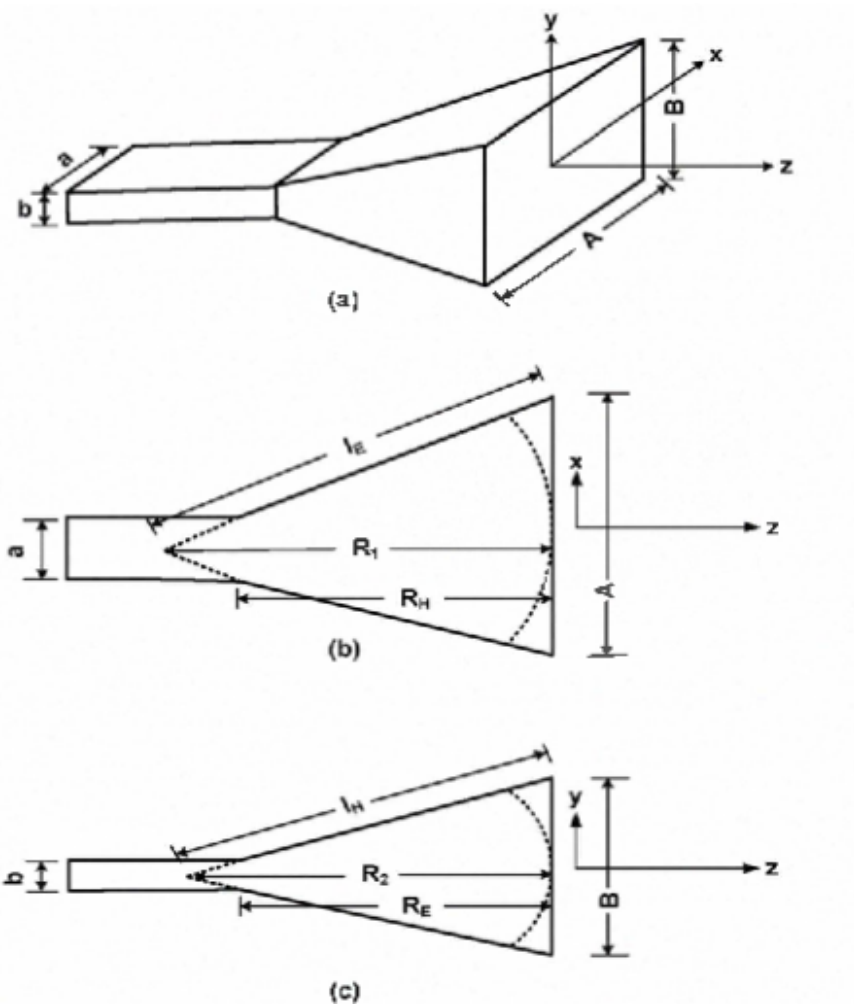


Figure 3: a. Overall geometry of pyramid horn antenna; b. E-field plane dimensions; c. H-field plane dimensions. Adapted from [2].

The last waveguide dimensions needed for this design is the distance between the back wall of the waveguide and the receiving probe, and the length of the waveguide. As the electromagnetic waves travel through the horn antenna and waveguide, it is essential that there is a conductive probe to focus and send the signals into the rest of the system.

This probe distance is calculated as being a quarter of the waveguide wavelength as shown via

$$\lambda_g = \frac{\lambda}{\sqrt{1 - (f_c/f)^2}} = 28 \text{ cm} \quad (1)$$

and

$$d = 0.25\lambda_g = 7 \text{ cm}, \quad (2)$$

where $f_c = 0.908$ GHz is the cut off frequency of the WR650 waveguide, and λ is the wavelength at the design center frequency f [5]. Lastly, the waveguide length is calculated to be 1.5 times the waveguide wavelength

$$l = 1.5\lambda_g = 42 \text{ cm}. \quad (3)$$

With all of the waveguide dimensions specified, the horn opening dimensions A and B are calculated via

$$A^4 - aA^3 + \frac{3bG\lambda^2}{8\pi\epsilon_{ap}}A = \frac{3G^2\lambda^4}{32\pi^2\epsilon_{ap}^2} \quad (4)$$

and

$$G = 0.51 \frac{4\pi}{\lambda^2} AB, \quad (5)$$

where G is the gain of the antenna and λ is the wavelength at f [2].

Solving for the roots of these equations, it is possible to plot dimensions A and B in meters against a specified gain G in dB. This plot can be seen in Figure 4. The plot has a referenced gain of 18 dB which has been shown by a similar project to be sufficient enough to receive hydrogen line radiation from celestial objects [6].

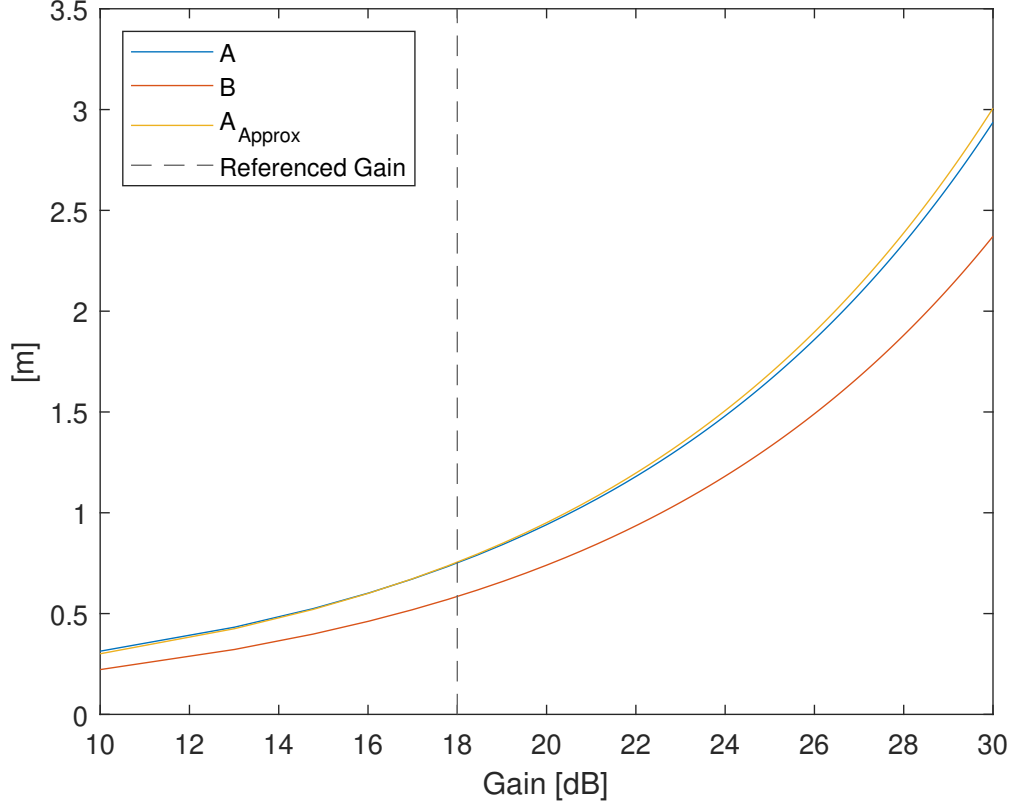


Figure 4: Horn dimensions A and B vs Gain.

With these values calculated, the remaining dimensions are calculated via

$$A = \sqrt{3\lambda R_1}, \quad (6a)$$

$$\frac{R_1}{R_H} = \frac{A/2}{A/2 - a/2} = \frac{A}{A - a}, \quad (6b)$$

$$l_H^2 = R_1^2 + \left(\frac{A}{2}\right)^2, \quad (6c)$$

$$B = \sqrt{2\lambda R_2}, \quad (6d)$$

$$\frac{R_2}{R_E} = \frac{B/2}{B/2 - b/2} = \frac{B}{B - b}, \quad (6e)$$

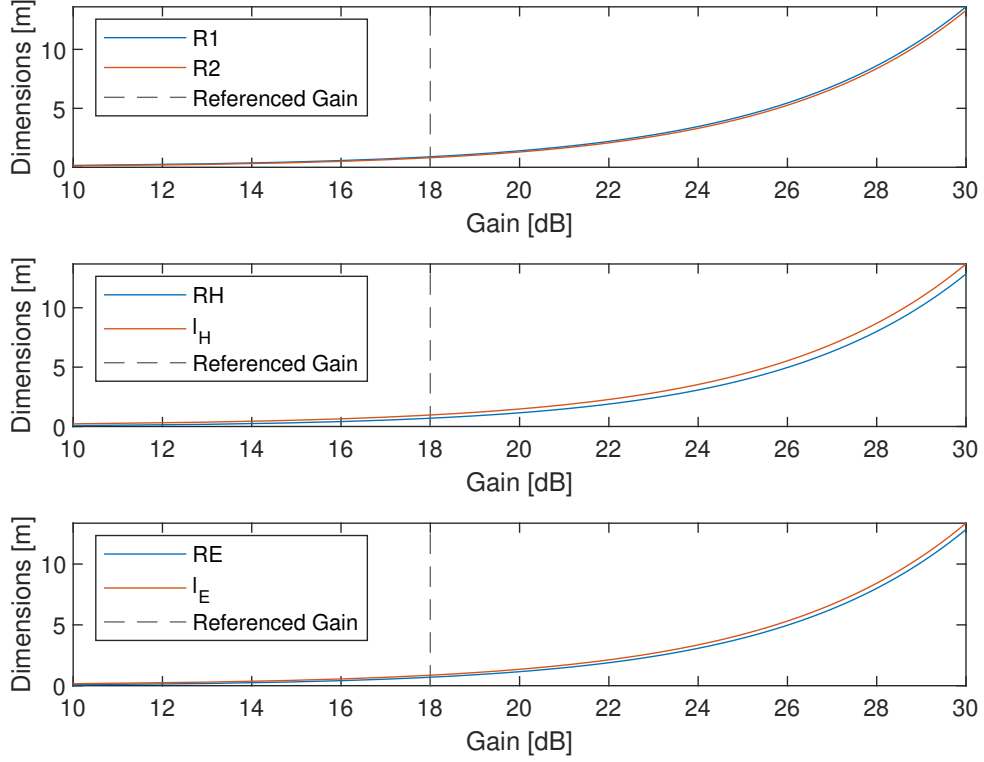


Figure 5: Secondary horn dimensions from Fig. 3b and 3c vs. Gain.

and

$$l_E^2 = R_2^2 + \left(\frac{B}{2}\right)^2. \quad (6f)$$

Using these equations, the plots of the dimensions compared to gain, G were created and can be seen in Fig. 5. Once again, the referenced gain level of 18 dB is used to select the design values. Lastly, the final pyramidal horn antenna dimensions are listed below in Tab. 1.

A	B	R_1	R_2	R_H	I_H	R_E	I_E
0.75 m	0.58 m	0.90 m	0.82 m	0.95 m	0.70 m	0.70 m	0.85 m

Table 1: Initial pyramidal horn antenna design dimensions.

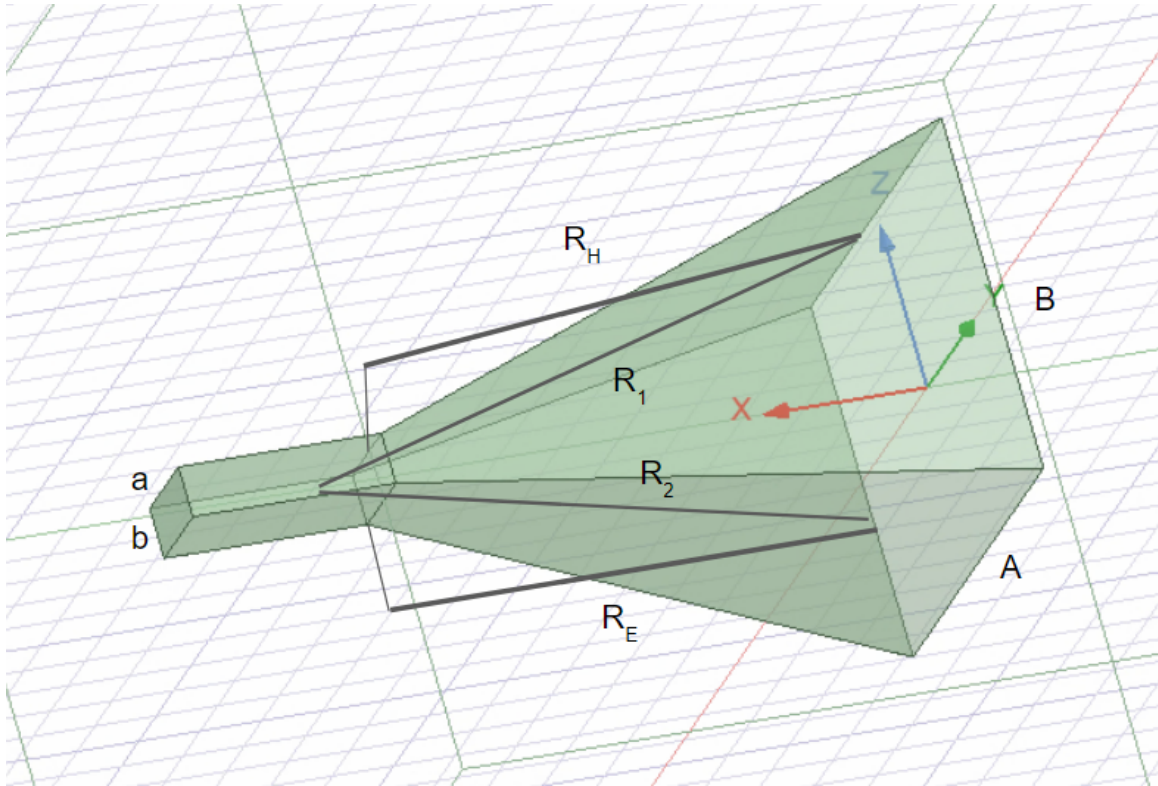


Figure 6: HFSS model of designed horn antenna with annotated dimensions.

2.1.2 HFSS Simulations

With all of the design specifications chosen, the next step was to verify them with HFSS simulations. A recreation of the designed horn can be seen in Figure 6.

Using this model, the directivity of the antenna is verified using a full wave simulation. Specifically, a far field approximation in HFSS can be used. This is done by setting an air box around the antenna to act as the radiation boundary. It is vital to ensure that the end of the waveguide section is terminated by this boundary so that the results closely align to this waveguide feeding into an open circuit. From this point, HFSS has a far field approximation of which the radiation pattern of the designed antenna can be extrapolated. Gain data from this simulation are shown in Fig. 7.

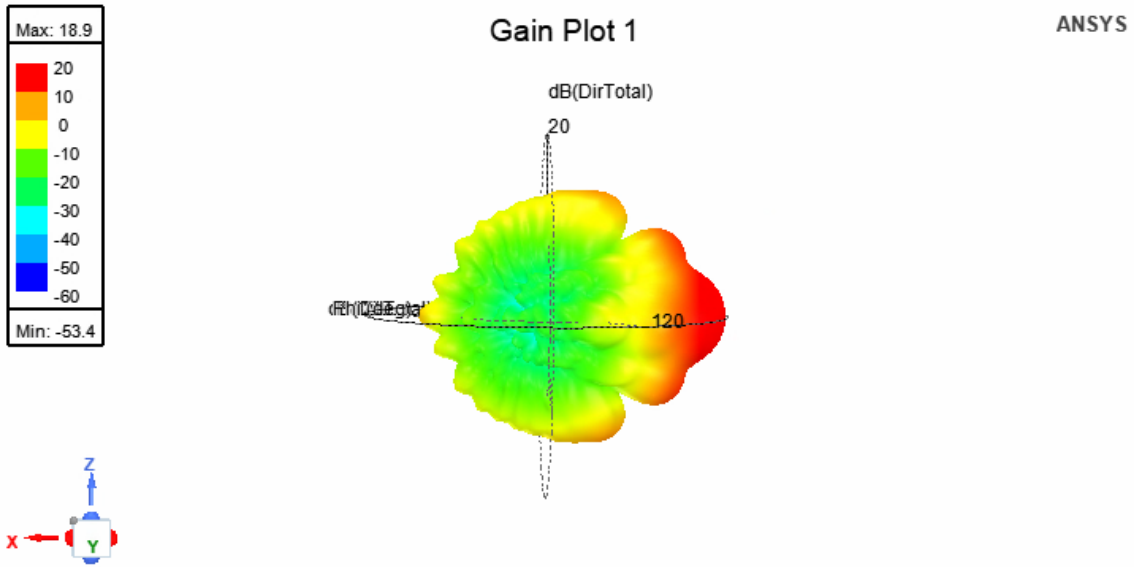


Figure 7: Simulated gain of HFSS model. Red lobes are the main lobes pointing in the direction of the opening of the horn.

An important verification that can be seen from the directivity simulation is that the designed system has a main lobe gain of 18.9 dB. As the antenna was originally designed to operate with 18 dB of gain, this plot confirms that the design is working as expected. With this in mind, the horn antenna can be constructed using these final design values.

2.1.3 Horn Antenna Construction

For the construction of the horn antenna, plywood is used for the shape and base of the antenna, and aluminum foil is used for the conductive surface of the antenna. The construction is split into two main sections, the pyramidal horn section, and the waveguide section.

The pyramidal horn section is created by cutting out the four faces from plywood sheets. Two of the faces are built with the dimensions of A and a as the widths, and R_H as the length. The other two faces use the dimensions of B and b as the widths,

and R_H as the length. The two different faces are connected to each other to create two “L” shaped combinations. The two combined pieces are then connected to create the pyramidal horn shape. Lastly, aluminum foil is taped with copper tape to the inside interfaces of the constructed horn.

As for the waveguide section, five faces were cut from the plywood sheets. Two of the faces have the dimensions of width a and length l . Another pair of faces have the dimensions of width b and length l . Lastly, the final face has the dimensions of a , and b . The four faces with the length of l are connected in the same manner as the pyramidal horn section. Aluminum foil is once again taped to the inside interfaces of the waveguide section.

With the waveguide section constructed, the next step is to create the probe interface. This is done by drilling a hole on the outside of one of the $a \times l$ faces that is $d = 7$ cm from its length-wise end. Note that this hole must be in the exact center of the face width-wise. The probe itself is created by connecting a wire, or in this project, a set of brass stand-offs to a SMA port. This probe is then connected such that the outer-jacket of the SMA connector is grounded to the aluminum foil, inner-jacket (the brass-standoffs) are not connected to the foil.

After the probe is installed, the final waveguide face ($a \times b$) is connected to the end of the waveguide (the side closer to the probe). Lastly, the waveguide and the pyramidal horn sections are connected together.

The constructed pyramidal horn section is shown in Fig. 8, the probe connection can be seen in Fig. 9, the constructed waveguide can be seen in Fig. 10, and the final combined horn antenna can be seen in Fig. 11

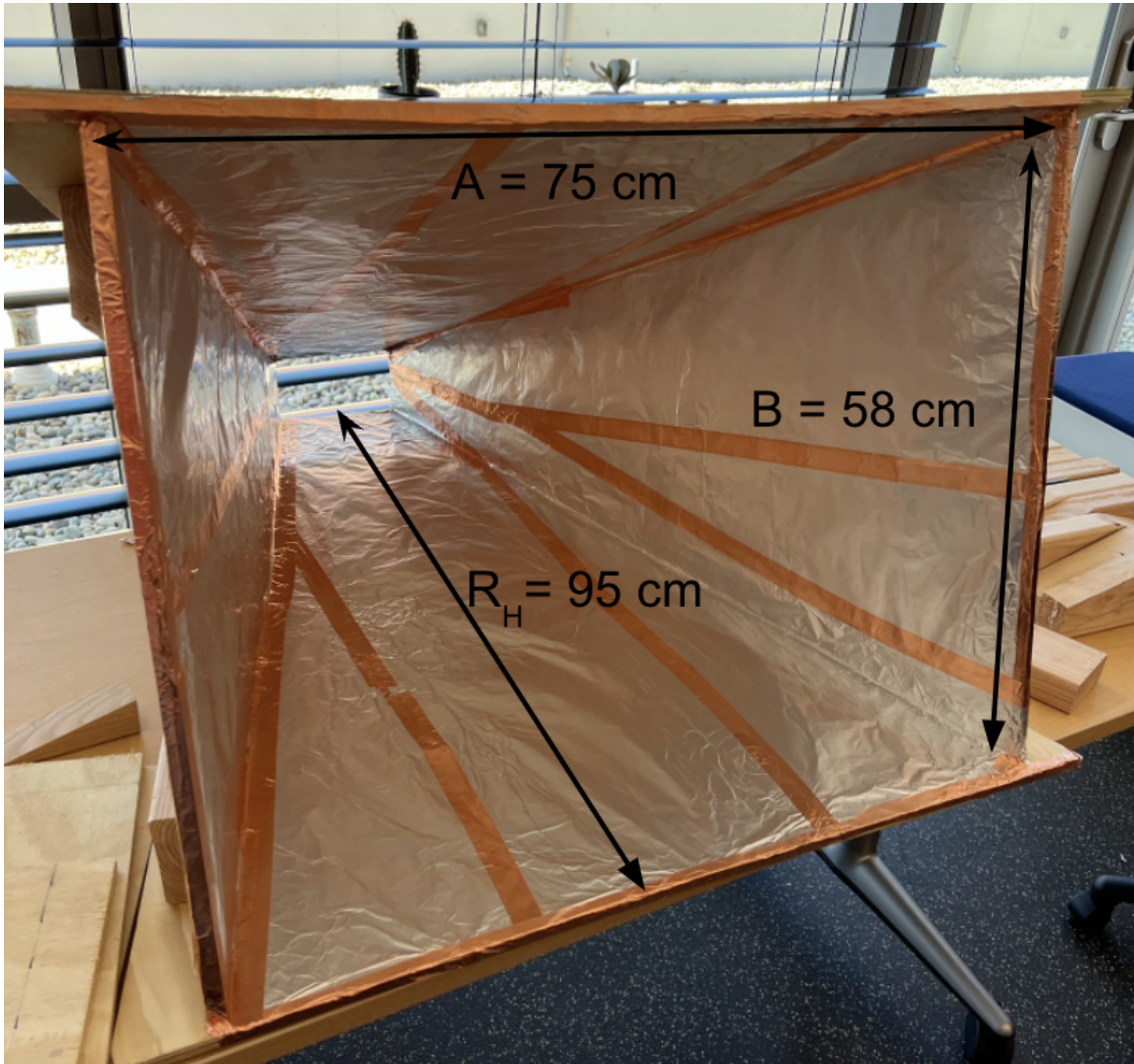


Figure 8: Constructed pyramidal horn section.



Figure 9: Waveguide probe connection.

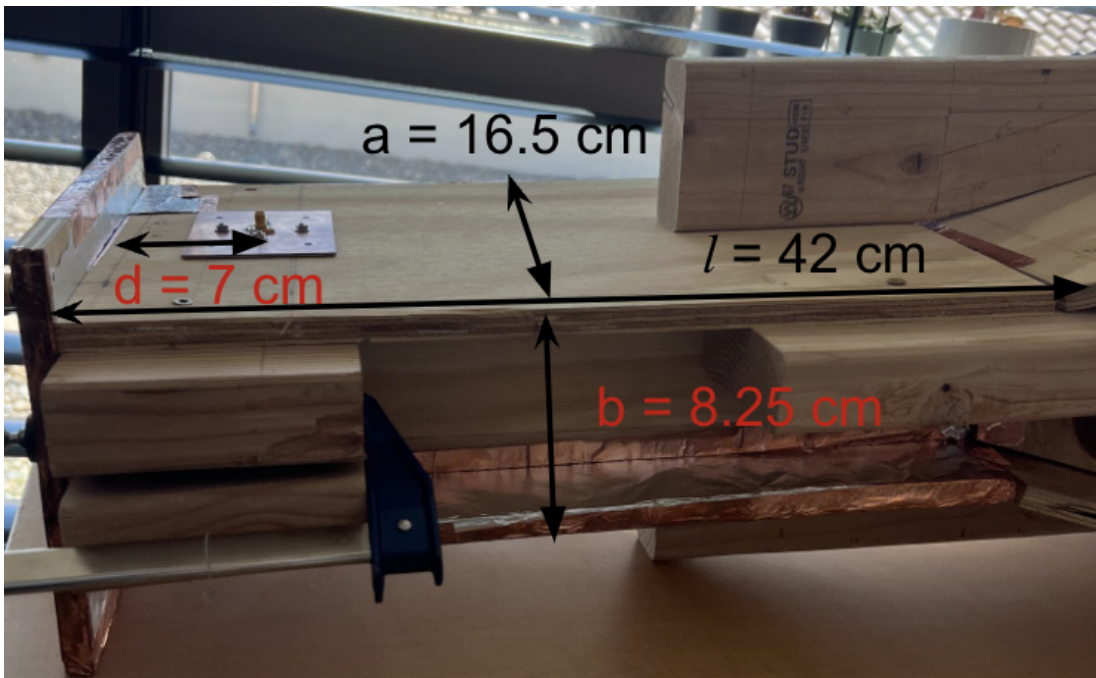


Figure 10: Constructed waveguide section.



Figure 11: Completely constructed pyramidal horn antenna.

2.2 Filters

2.2.1 Filtering Topologies

The radio astronomy band is between 1400 - 1427 MHz. We expect to see hydrogen radiation sit between this band. Furthermore, it is also the FCC allocated band for this application. To receive these signals with a high SINR (Signal to Interference & Noise Ratio), the signals of other frequencies must be sufficiently filtered.

To begin our filter design, we must examine different filter topologies and compare their design, ease of construction, and finally their results. Two topologies that are immediately apparent are the coupled line bandpass filter and the lumped element bandpass filter. The coupled line bandpass filter is implemented using microstrip lines configured in a specific layout that is specified using design equations [3]. The lumped element bandpass filter is implemented using inductors and capacitors to emulate the same behavior.

2.2.2 Coupled Line Filter Design

Coupled line filters use a microstrip line implementation. These implementations follow the structure as seen in Fig. 12, where each grey, rectangular section represents a coupled microstrip line. Each coupled line has two different impedances used for calculation. These are denoted by Z_{0e} and Z_{0o} . These impedances correspond to “even” and “odd” impedances. The important geometric parameters of these filters are the lengths and widths of each line, as well as the spacing in between each coupled section. To begin these calculations we’ll start by calculating values for admittance converters.

$$J_1 = \frac{1}{Z_0} \sqrt{\frac{\pi \Delta}{2g_1}} \quad (7a)$$

$$J_n = \frac{1}{Z_0} \frac{\pi \Delta}{2\sqrt{g_{n-1}g_n}} \quad (7b)$$

$$J_{N+1} = \frac{1}{Z_0} \sqrt{\frac{\pi \Delta}{2g_N g_{N+1}}} \quad (7c)$$

Where values of J denote the equivalent admittance inverter values of the design and N denotes the order of the filter. Δ represents our fractional bandwidth, and different values of g_n are constant element values for a low-pass filter prototype. The next step is to calculate the impedance values of each coupled line section. These calculations use the admittance inverter values found above.

$$Z_{0e} = Z_0[1 + JZ_0 + (JZ_0)^2] \quad (8a)$$

$$Z_{0o} = Z_0[1 - JZ_0 + (JZ_0)^2] \quad (8b)$$

Where Z_{0e} and Z_{0o} are the even and odd impedances of a coupled line section. Finally, we will calculate the widths of these lines.

$$\frac{W}{h} < 1 : Z = \frac{Z_0}{2\pi\sqrt{\epsilon_{eff}}} \ln\left(\frac{8h}{W} + \frac{W}{4h}\right) \quad (9)$$

$$\frac{W}{h} > 1 : Z = \frac{Z_0}{\sqrt{\epsilon_{eff}} \left[\frac{W}{h} + 1.393 + 0.667 \ln\left(\frac{W}{h} + 1.444\right) \right]} \quad (10)$$

Where W is the width of the line, h is the substrate height, Z_0 is the given port impedance, and ϵ_{eff} is the effective permittivity of the substrate. For our filter design, we will set our coupled line lengths at a quarter wavelength. Coupled line filters of order N have $N + 1$ coupled sections. Therefore, the filter seen in Fig. 12 is a 6th order filter design.

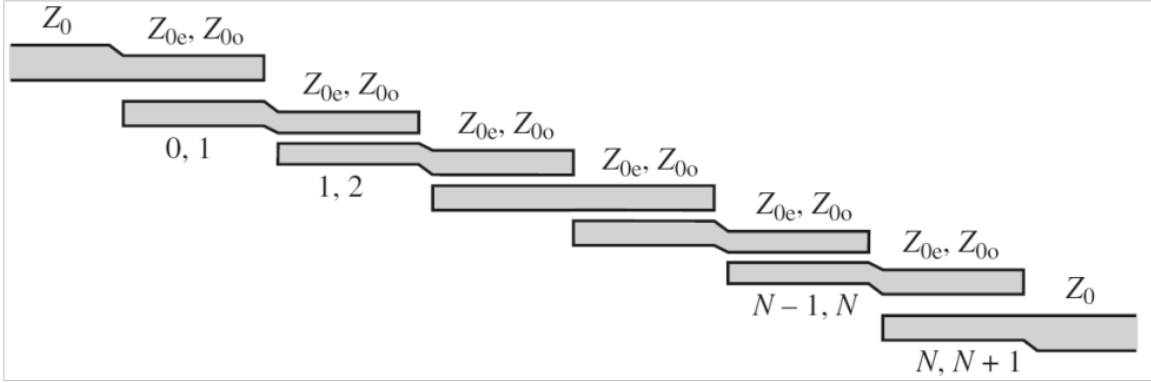


Figure 12: Coupled line filter layout

2.2.3 Lumped Element Filter Design

The lumped element bandpass filter is implemented using a configuration of capacitors and inductors. The methodology of constructing this design is to begin with a low-pass filter prototype using the same constant element values for a low-pass filter prototype as mentioned in the coupled line filter design. The low pass filter prototype utilizes series inductors and shunt capacitors.

To transform this low-pass filter prototype into a bandpass filter we must replace each series inductor with an inductor in series with a capacitor and replace each shunt capacitor with an inductor in parallel with a capacitor. A 3rd order bandpass filter transformation is seen in Fig. 13, where each series inductor and capacitor was originally a single inductor and each parallel inductor and capacitor was originally a single capacitor. The values of these inductors and capacitors are obtained via

$$L'_k = \frac{g_k Z_0}{\omega_0 \Delta} \quad (11a)$$

$$C'_k = \frac{\Delta}{\omega_0 g_k Z_0}, \quad (11b)$$

where g_k denotes the k th value of the constant element values, Δ represents the fractional bandwidth, ω_0 is the center frequency, and Z_0 is the port impedance of our

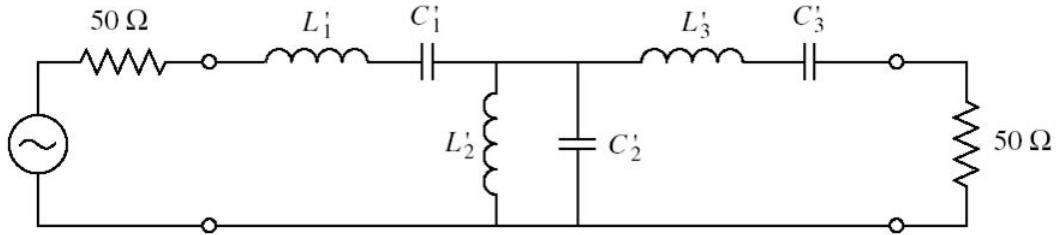


Figure 13: Lumped element bandpass filter. Adapted from [3].

system.

2.3 Software Defined Radio and Data Processing

2.3.1 GNU Radio Installation

As a group, we decided to use GNU Radio as our software framework for all of our Software Defined Radio (SDR) applications. GNU Radio is a free open-source framework toolkit that uses Python3 as a base. It features a streamlined method of creating various blocks required in an SDR. These are called flow-graphs, which allow filters and other methods of signal processing to be easily manipulated. The two SDR candidates we decided upon were the RTL-SDR Blog V3 and the Ettus B210. The purchased SDRs also provide official software support and resources to use the SDRs on GNU Radio.

Our first installation of GNU Radio was easy to complete; the tutorial provided by GNU Radio was well documented for any types of errors. After trying various established radio astronomy flowgraphs for GNU Radio, it seemed that once the two

SDRs we designated were purchased, that it would be a smooth process to program a new flowgraph that would allow our SDRs to receive and plot the 1420 MHz center frequency from our horn antenna.

As an open source software, GNU Radio allows various packages to be installed to facilitate the use of various SDRs. The largest problem is that certain packages must be installed before GNU Radio is installed, which is not immediately apparent. The first SDR to arrive was the RTL-SDR Blog V3, which is a small, inexpensive SDR to provide amateur radio astronomers access to a purpose built SDR. Provided with the SDR is a build script that re-installs GNU Radio with the RTL-SDR Blog package. Afterwards, the higher quality SDR, the Ettus B210, was arrived to be setup in our system. The Ettus B210 provides a very detailed method of installing their packages. Upon installing the package, it is easy to start using the SDR as an input in the flowgraph centered around 1420 MHz. Installing just the package is not enough for this SDR; the Ettus B210 is a higher grade SDR compared to the RTL-SDR Blog V3 and thus has a Field Programmable Gate Array (FPGA) on its PCB. Unlike CPUs, the integrated circuitry inside an FPGA is routed via an FPGA image, which is a bit-stream that assigns interconnects to the logic blocks which ultimately produces the FPGA's overall function. Thus, we met errors when using the Ettus B210 until we used a script that reproduced the manufacturer's FPGA images [7]. Those FPGA images are then compared to the ones that are loaded by factory default on the Ettus B210, and once they are confirmed to be the same the SDR functions similarly to the RTL-SDR Blog V3.

2.3.2 Recording Packets and Plot Generation

Black-body radiation from hydrogen is affected by the Doppler effect, and so the SDR should plot signals over time to display that change. The SDR produces frequency spectra over an allocated time frame. Computer storage for the signals recorded by the SDR is somewhat limited in the sense that an average of 200 Megabytes of data

is recorded for each 100 milliseconds of a recorded signal. If the computer runs out of memory during a recording session, the remaining recording time will be lost. To accommodate the long recording sessions of longer than eight hours for the radio telescope, the recording time needs to be subdivided into packets that still bring enough data to analyze. Recording for eight hours with packets the length of 100 milliseconds still results in approximately 96 Gigabytes of data, but that amount avoids any memory issues during recording sessions.

After using the SDR to record the 100 millisecond bursts, a fast Fourier transform (FFT) is performed on each packet is created so the center frequency of the hydrogen recorded at that specific time can be denoted. Instead of having an FFT plotted separately, an FFT is graphed as a single line with the intensity at each frequency graphed according to a color scale. Once each FFT is performed, they are layered in order of time created such that the oldest signals are lined at the top and the most recent signals are at the bottom. This creates a 3D graph known as a waterfall plot. A sample of the waterfall plots created by the packet reading script can be seen in our test section in Fig. 24. By looking at a waterfall plot, we can determine how a celestial body moves if the center frequency at a packet is offset from 1420 MHz due to the Doppler effect.

3 Project Outcomes

3.1 Antenna and Waveguide

To verify the performance of the constructed pyramidal horn antenna system, there are two main tests to be conducted. The first is to test how well the impedance of the antenna is matched, and the second is to test the directivity of the antenna.

3.1.1 Impedance Match Verification

To verify the match of the antenna, a one port reflection coefficient measurement is taken. The reflection coefficient S_{11} is a value that shows the ratio of power going into port 1 vs. power going out from port 1, i.e.,

$$S_{11} = P_1^- / P_1^+. \quad (12)$$

This is a significant metric as it describes how much power is being reflected back into the system. As this reflected power is being lost from the received signals, it is desired to have this reflection be as low as possible.

This test is conducted by connecting the output of the antenna to a Network Analyzer which then runs the S_{11} measurement over a specified frequency range. The test set up can be seen in Fig. 14, and the results the test can be seen in Fig. 15.

The important take-away from this test is the S_{11} value at the design frequency, $f = 1420$ MHz as indicated by the dashed line on the plot. From this, it is seen that S_{11} is around -10 dB at this frequency, or 0.1 in linear scale. What this signifies is that the designed horn antenna loses 10% power due to a mismatch in impedance. It is also interesting to note that the impedance test shows that there seems to be a better match (more negative S_{11}) for a frequency of around 1550 MHz. With further tweaking of the set-up, it would likely be possible to move this behavior towards the intended design frequency and improve the match of the antenna. However, this



Figure 14: Horn antenna connected to Fieldfox Network Analyzer for impedance test.

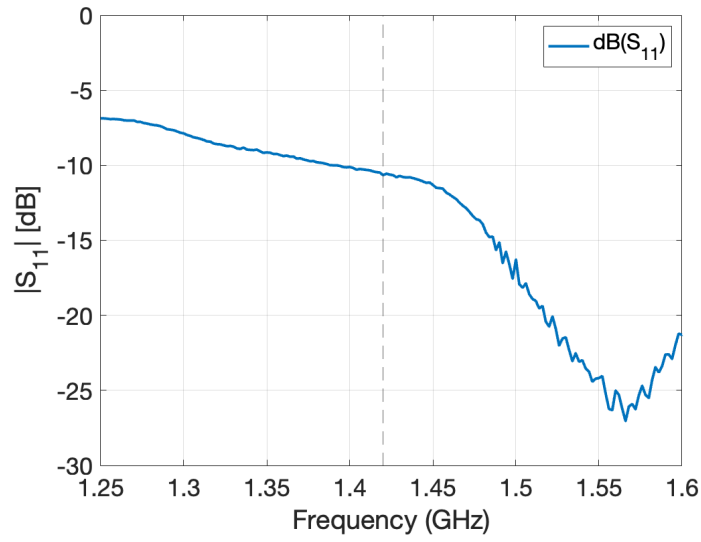


Figure 15: S_{11} vs. Frequency of constructed horn antenna.

would result in only a marginal increase in performance (less than 10%) and was decided to be not worth pursuing for the scope of this project.

3.1.2 Antenna Directivity Verification

Another important aspect of the designed antenna that needs to be verified is its gain and directivity. This is a metric of how much the antenna amplifies signals at certain points of its surrounding aperture. For this project, it is vital that the designed antenna has a high directivity in its direct line of sight (main lobe) and a low directivity elsewhere (side lobes). This behavior is desired because the signals to be received are low power signals and the telescope needs to be able to distinguish them from surrounding noise. The directivity tells how much the antenna's radiated power is focused in a single direction, while the gain shows how efficient the antenna is at radiating power in this direction.

The directivity test is conducted by using a RF signal generator and a separate antenna to transmit a test signal over-the-air into the pyramidal horn antenna. The transmit antenna is then moved in different angle increments away from the direct line of sight (0°) at the same height (lateral angle of 0°). At each marking, the received power at the center frequency $f = 1420$ MHz is recorded. This testing set up can be seen in Fig. 16

With this set of experimental data collected, it is possible to compare it to the HFSS simulated directivity in order to verify the performance of the constructed antenna. To do so, the set of data from the HFSS radiation plot that refers to a lateral angle of 0° with differing azimuth angle is overlaid on top of the experimental results. It is important to note that since there are nonidealities in the transmitting antenna and loss from over-the-air transmission, the experimental data needs to be normalized to the same scale as the simulated data in order to be compared properly. The resulting comparison plot can be seen in Fig. 17.



Figure 16: Directivity test set up, tape markings denote different angle measurement placement.

Fig. 17 shows that the constructed horn antenna's directivity aligns closely to the expected simulation results. While there are slight discrepancies at each point, the general trend of having higher gain at direct line of sight and lower gain at side angles is observed.

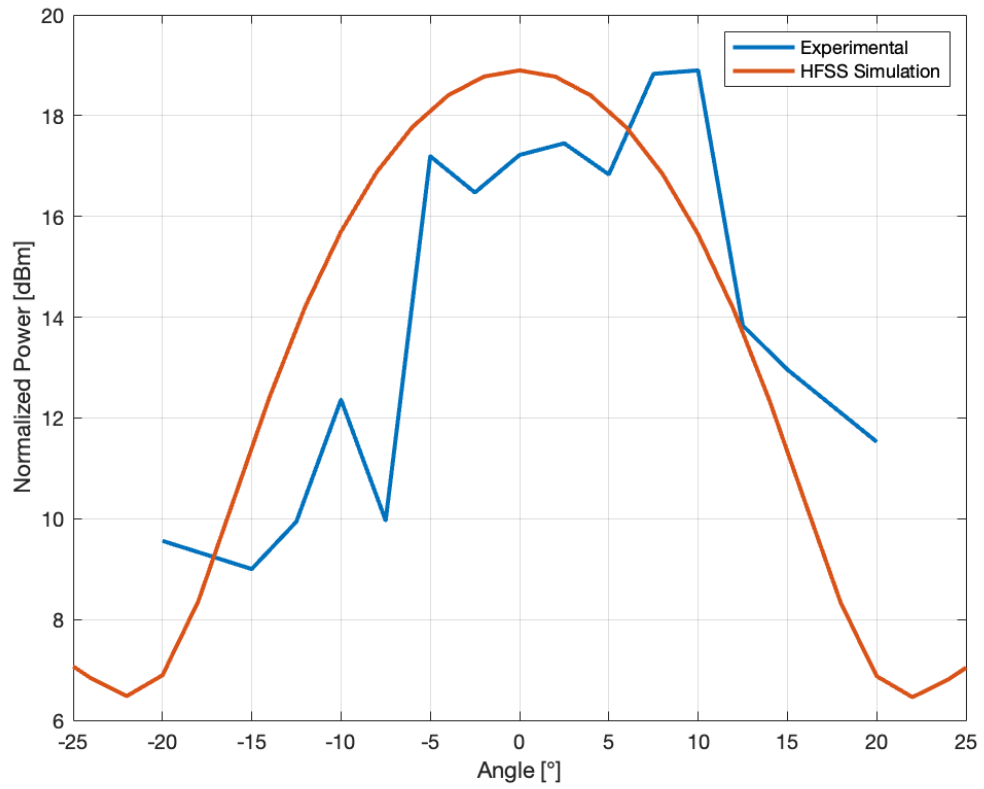


Figure 17: Normalized power vs. Azimuth angle for HFSS simulation and the over-the-air experiment.

3.2 Filters and Amplifiers

3.2.1 Filter Implementation

With a coupled line and lumped element bandpass filter design completed, the choice of implementation will be decided on the ease of construction as well as the robustness of the design itself. The lumped element filter design equations realize values for inductors and capacitors that can be much too specific and have non-standard values. As a result, you are limited by the element values you can find online to purchase. This causes a host of purchasing problems as well as performance issues. Furthermore, the construction of a lumped element filter can be difficult without extensive soldering experience.

On the other hand, a coupled line filter is much easier to construct using the print and etching process. Additionally, it is much easier to come closer to precise width and length values of a coupled line than of lumped element values. As a result, there will be less performance issues.

After these considerations, a coupled line filter will be chosen as the preferred implementation.

3.2.2 Coupled Line Filter Robustness

With the coupled line filter chosen, a manufacturing robustness test will need to be run before a design is constructed. This is done with a Monte Carlo simulation, which adds a specified level of deviation to the components and therefore shows how much manufacturing error our filter will tolerate. These errors were put onto lengths and widths of the microstrip lines as these are the areas we would expect to see such deviations from manufacturing. The plot in Fig. 18 shows a histogram of these simulations for 4th and 7th order filters. The bins inside the yellow highlighted area do not meet our specified level gain of -5 dB at the center frequency and the bins to the right of this section do meet our specified level of gain.

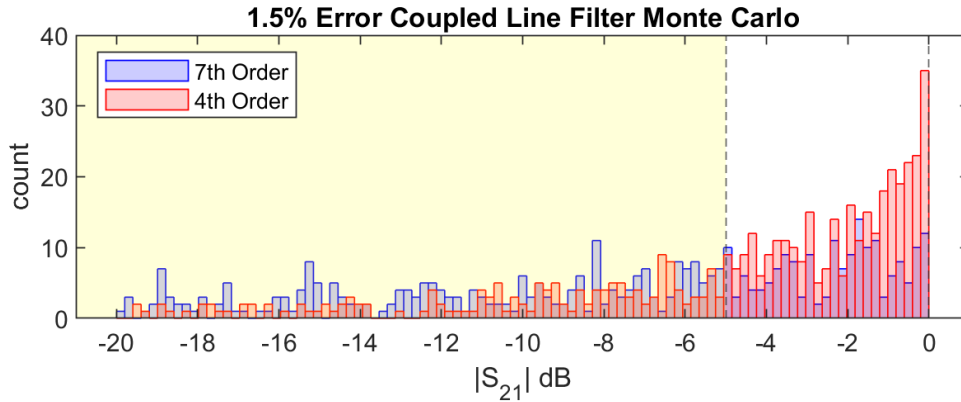


Figure 18: 4th & 7th order coupled line filter performance histogram

Although a 7th order filter would provide us with much better filtering, such as a faster frequency response and steeper roll-off, the histogram shows how much more robust the 4th order filter will be. The 4th order filter yields a nearly 90% manufacturing success rate with 1.5 % error.

3.2.3 Amplifier Gain Tests

With three Low Noise Amplifiers purchased, we must now test the performance of each. An amplifier gain test is the most important and relevant test for these amplifiers. This test will be done using a network analyzer. Checking the results of the S_{21} parameters for each amplifier will tell us the gain seen at the output port 2 relative to the input port 1. The results of these tests are seen in Fig. 19.

Fig. 19 shows the gain performance of two general purpose amplifiers which are highlighted in yellow and red. These amplifiers are considered general purpose due to their high level of gain across the entire frequency range. On the other hand, the purpose built amplifier shown in blue only has a high level of gain in the frequency band of interest. This highly varying level of gain across the frequency spectrum is the result of built in filtering within this amplifier. This filtering allows for the amplifier to have a gain as high as 40 dB in the frequency band of interest and at the

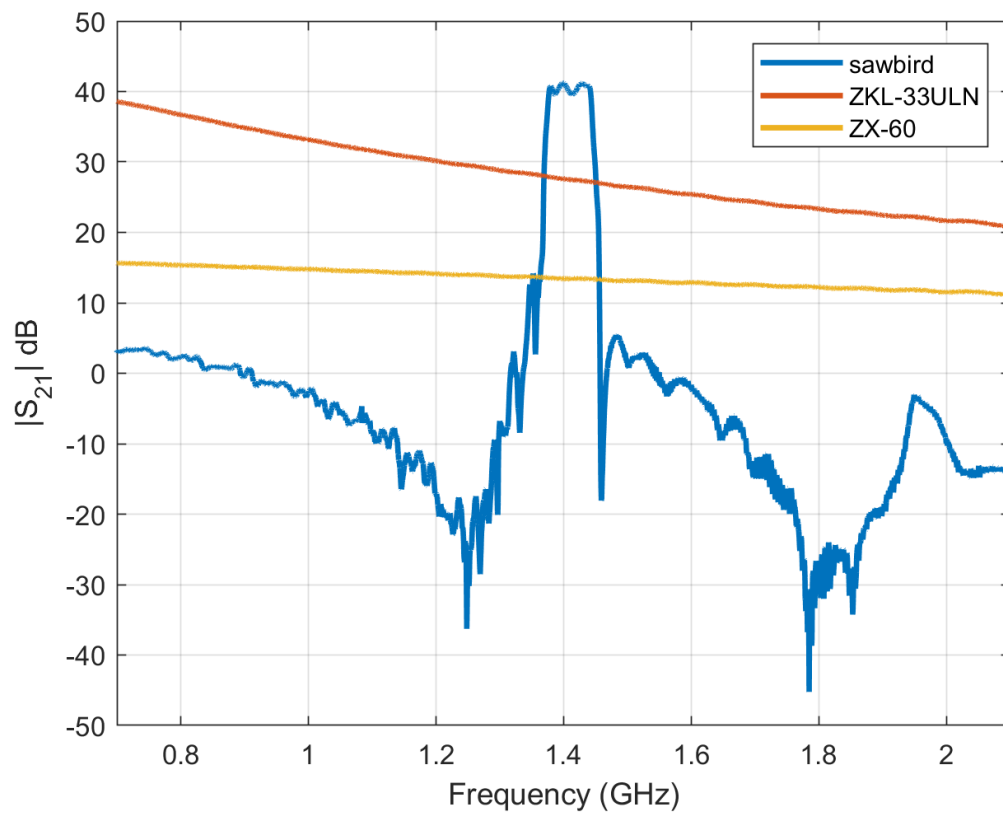


Figure 19: Amplifier Gain Comparison

same time have a gain of 0 dB or less everywhere else. Not only does the SAWbird amplifier have the highest level of gain at the center frequency, but it also has sufficient filtering. The SAWbird amplifier is therefore the logical choice of implementation for the radio telescope. Furthermore, the project can save on costs with the SAWbird implementation since a coupled line filter need not be constructed due to the sufficient level of filtering from the amplifier.

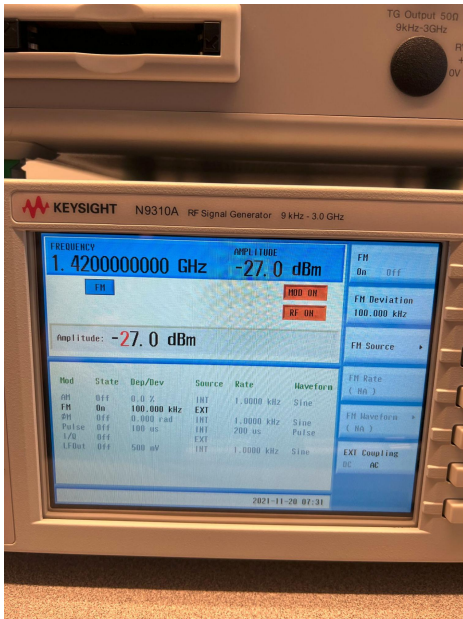
3.3 Software Defined Radio and Data Processing

Before integrating the whole system together, verification that the SDRs purchased can receive radio signals at 1420 MHz is required. To reiterate, 1420 MHz is the typical center frequency for the black-body radiation of hydrogen surrounding celestial bodies, and so we want to see the SDRs capability of reading that frequency.

The RF Signal Generator in Fig. 20a is the main instrument of our test bench, which creates a 1420 MHz signal that acts as our black-body radiation input for the SDRs. We attach an Arbitrary Waveform Generator in Fig. 20b as an external source so that we can have a lower frequency modulation (FM) deviation on our RF Signal Generator. By changing the amplitude on the Waveform Generator we can have a large amplitude like in Figure 21 or a smaller amplitude like in Fig. 22. The last part of our test equipment is the Spectrum Analyzer in Fig. 20c, which we use as a secondary input from the RF Signal Generator to check that the signal is below -20 dB before plugging it into our SDRs. The Spectrum Analyzer also serves as a way to compare its plot to the plots of the SDRs'.

Although the FM deviation's amplitude is different for Fig. 21 and Fig. 22, all other parameters are the same. The top graph of both figures is the waterfall plot of our input signal. The waterfall plot is a plot of time in seconds against frequency in MHz. The relative gain on the waterfall plot is shown by color, which is a spectrum from blue as low relative gain to red as high relative gain. When we reference the

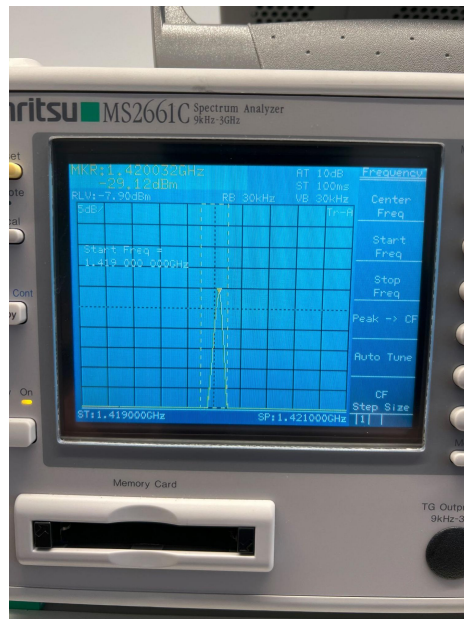
bottom plot of both figures, which plots relative gain to frequency, we can deduce why areas on the waterfall plot are a certain color. The RTL-SDR Blog V3 SDR is a much cheaper SDR, and thus the signal's noise levels are relatively high to the center frequency we are trying to get. This produces a large sea of green on the waterfall plot, around the orange wave. The Ettus B210, which uses its higher cost to incorporate many tools to filter out the noise such as the on-board FPGA, shows a much lower gain from noise and thus the waterfall plot produces a sea of blue around our signal. When comparing our SDRs, we can see that the RTL-SDR Blog V3 still produces the waterfall plots we want in Radio Astronomy at a low cost, but the more expensive Ettus B210 shows superior noise characteristics.



(a) Keysight N9310A RF Signal Generator used to generate test signals for verifying SDR functionality.



(b) Agilent 33220A Arbitrary Waveform Generator used to add a lower frequency FM deviation.



(c) Spectrum Analyzer for verifying test signals.

Figure 20: RF Test Signal Setup

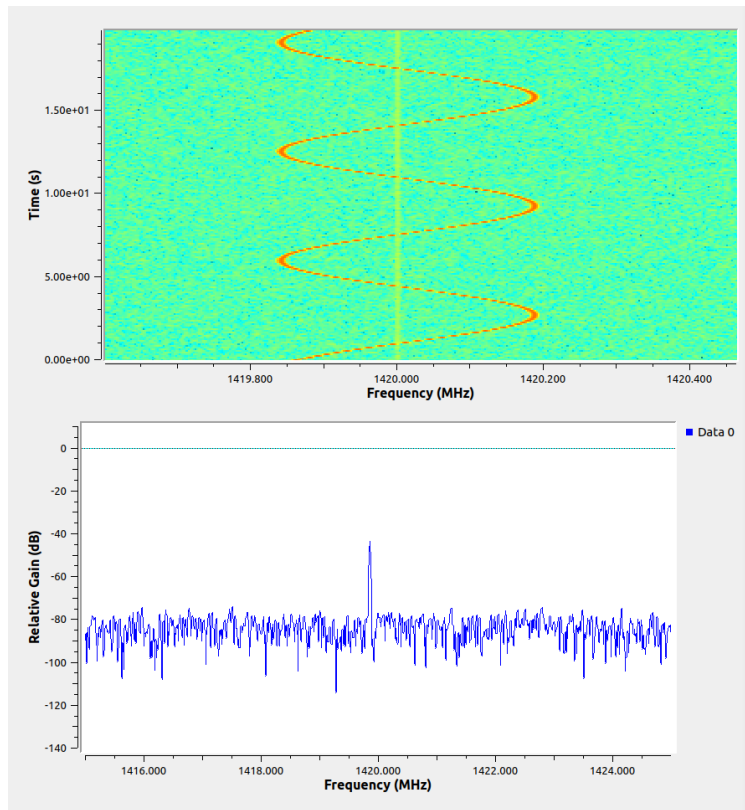


Figure 21: RTL-SDR Blog V3 Waterfall Plot and Spectrum Analysis.

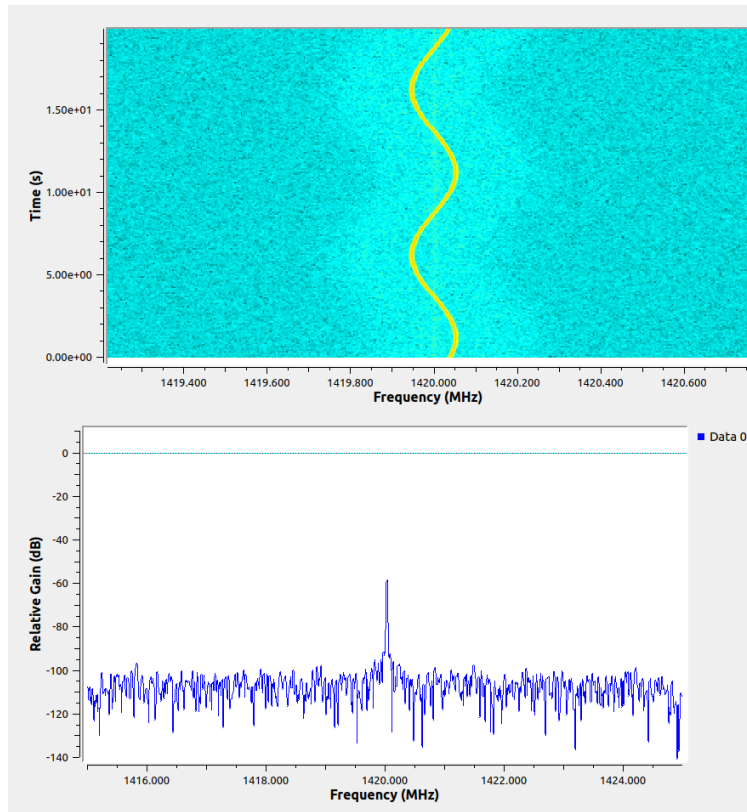
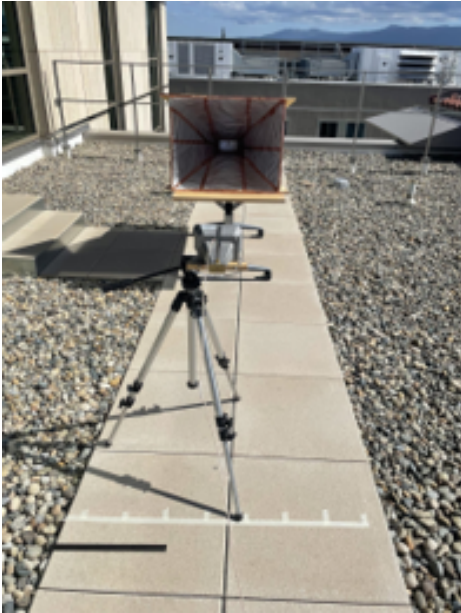


Figure 22: Ettus B210 Waterfall Plot and Spectrum Analysis.

3.4 Full System Trials

The full system setup is depicted in Fig. 23. A signal is received by our manufactured Horn Antenna, amplified by the SAWbird LNA, and finally processed by the SDR. To test the packet recording capabilities in the full system, we sent a signal from another horn antenna to our entire system at 1420 MHz -67 dBm with modulation at 15 mHz and 700 mV. This signal emulates black-body radiation from hydrogen atoms in space, but at the same time the signal's modulation speed is significantly faster than what is expected when scanning the sky for celestial bodies. To reiterate, modulation creates an oscillation in the signal that replicates the capability to acquire Doppler shifts. By the Doppler effect, a center frequency of higher than 1420 MHz will be a blue shift as in the object is moving closer to Earth. A red shift occurs when the center frequency of the signal is less than 1420 MHz, which means the object is moving farther away from Earth. Thus, each recording burst of 100 milliseconds are tested at two different intervals, one second in Fig. 24 and five seconds in Fig. 25.

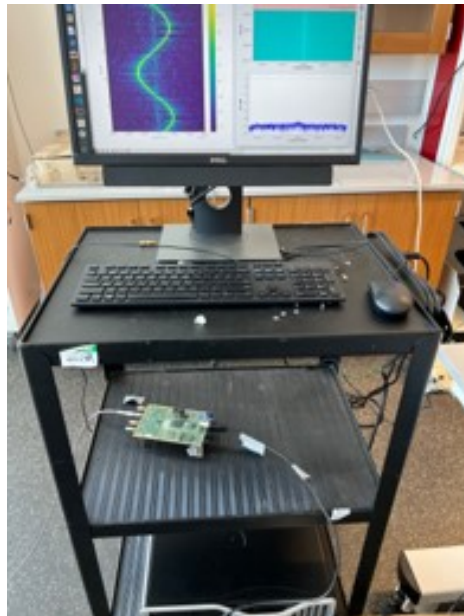
The x-axis of these waterfall plots is the frequency, with the color scale representing the intensity in dBm of the signal. The y-axis describes what time that signal was received from the start. Fig. 24 demonstrates a higher resolution depiction of the modulated wave because each packet is created within one second of each other. Although seeing the full modulated wave can help us more precisely determine characteristics of a celestial body's motion, the high expense of computing power and storage makes this detailed graph unnecessary. Furthermore, the signal's oscillation is significantly faster than what is typically in space. Fig. 25 which for the same time interval has packets created at 1/5th the rate can still keep up with the overall trends for the signal oscillation, while saving on computing power and storage. So, if this low packet recording interval is used on the slow changes from hydrogen signals emitted from space, it will be more than enough to analyze the direction at which objects move in space.



(a) Signal received by Antenna



(b) Coaxial feed to LNA input.



(c) SDR receiving and processing.

Figure 23: Full System Setup

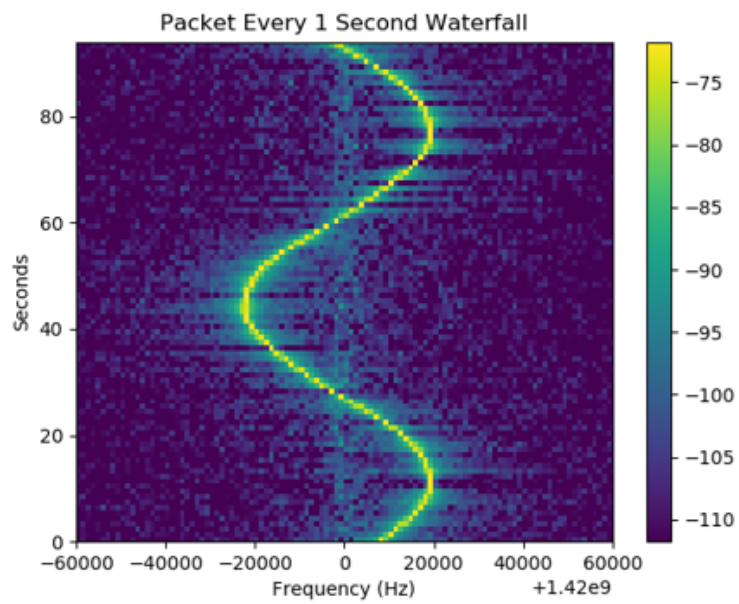


Figure 24: Recording modulated 1420MHz test signal over the air every second.

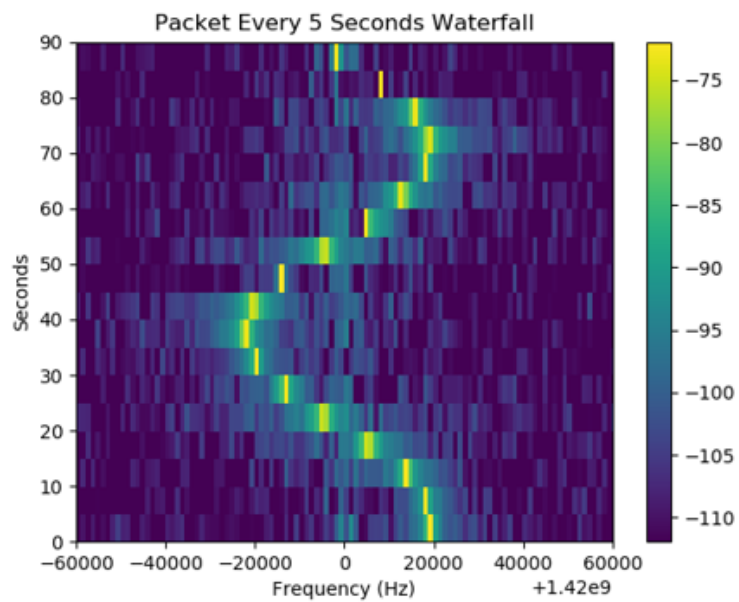


Figure 25: Recording the same modulated 1420MHz test signal over the air every 5 seconds.

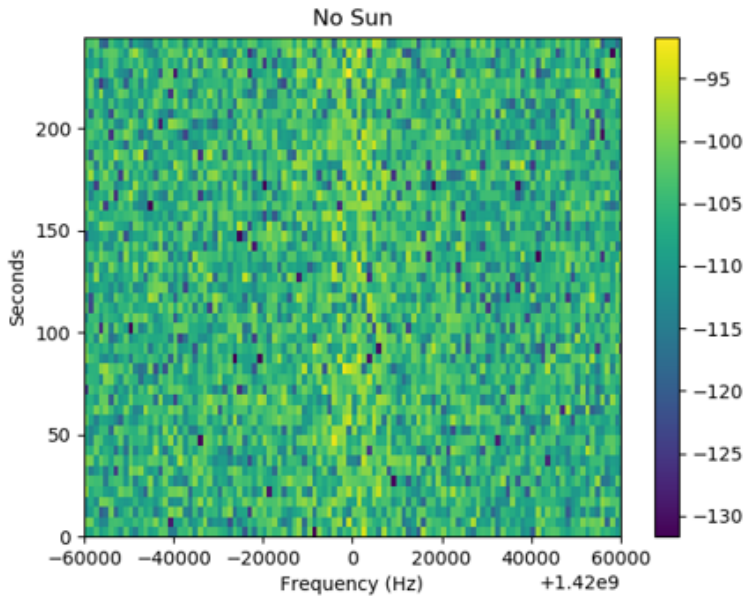


Figure 26: Antenna pointing to empty space.

The final trial is observing a celestial body. We set up a control recording in the form of scanning empty space as seen in Fig. 26. The anticipated difference between a signal with empty space and a signal pointing at the Sun should be a higher intensity in dBm shown on the color bar for the signal with the Sun on the waterfall plot. After recording each experiment, there appears to be little to no difference in the received signal from the Sun when compared to empty space. More fine tuning to the antenna and digital signal processing will be needed by a future team to properly acquire the Sun.

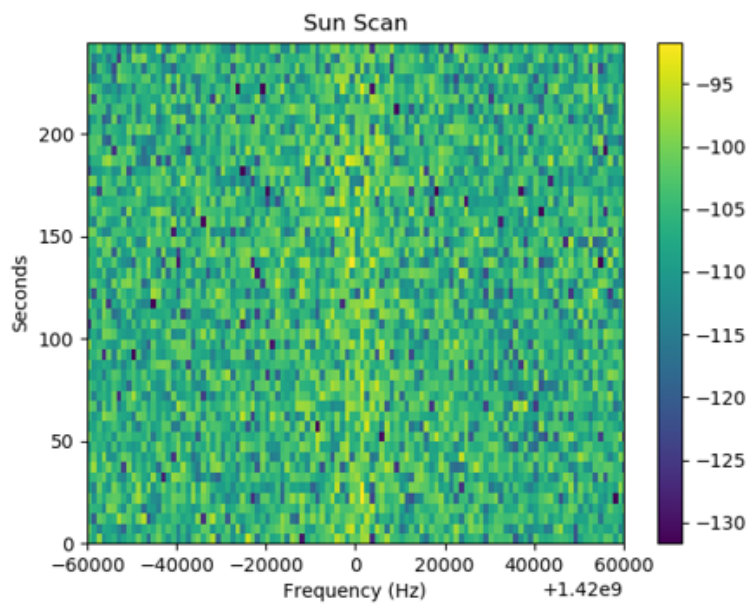


Figure 27: Antenna pointing to the Sun.

4 Conclusion

4.1 Final Design Assessment

In conclusion, the designed Radio Telescope system is able to successfully receive and create plots from artificial H-line signals transmitted over-the-air. All of the completed modules have been tested and verified both individually and combined. The only objective that the project is unable to achieve is to be able to receive and plot actual signals from celestial bodies in the galaxy. Despite this, the project is a successful prototype and proof-of-concept for radio astronomy capabilities at SCU.

4.2 Concluding Thoughts and Future Work

As this project is just the first stage of a multi-year project, all of the design considerations, results, and findings will be passed down to a subsequent senior design team. For the next stage of the project, we plan to move on from the pyramidal horn antenna topology to a parabolic dish antenna. We also hope to build a physical steering system that can automatically point the antenna to a specific object in the sky. Lastly, we want to further examine the digital signal processing that the SDR is performing to ensure that we are reading the data correctly. We are excited with the current progress in our radio astronomy project, and look forward to seeing a completed SCU radio telescope in the future.

References

- [1] B. I. Supriyatno, T. Hidayat, A. B. Susksmono, and A. Munir, “Development of radio telescope receiver based on gnu radio and usrp,” in *2015 1st International Conference on Wireless and Telematics (ICWT)*, 2015, pp. 1–4.
- [2] W. L. Stutzman and G. A. Thiele, *Antenna Theory and Design*. Wiley, 2013.
- [3] D. M. Pozar, *Microwave Engineering*. Wiley, 2013.
- [4] “Waveguide sizes.” [Online]. Available: <https://www.everythingrf.com/tech-resources/waveguides-sizes>
- [5] “Waveguide mathematics.” [Online]. Available: <https://www.microwaves101.com/encyclopedias/waveguide-mathematics>
- [6] E. Trumbauer and S. Khashayar, “Lightwork memo 29: Hydrogen line project documentation,” Jan 2021. [Online]. Available: <http://wvurail.org/lightwork/memos/LightWorkMemo029-r2-HydrogenLineProject.pdf>
- [7] “Usrp hardware driver and usrp manual.” [Online]. Available: https://files.ettus.com/manual/md_fpga.html

A Appendix

A.1 Equipment List

The overall list of equipment and budget for the project can be seen below in Tab. 2. The items column of this table is distinguished between SDRs, amplifiers, and antenna materials. The second column includes the part names and the final column includes the pricing of each individual part. Finally, the bottom of the table includes the total budget of our project.

Each device was selected based on their ability to perform within our selected bandwidth between 1400 - 1427 MHz as well as their low noise figures. The signals from space are small, so low noise figures are a must. The USRP B210 is an SDR with a performance between 1-6 GHz, which contains the 1420 MHz center frequency of interest. This same specification was made for the RTL SDR Blog V3, which is an SDR built as a budget friendly option in this band but at the cost of higher noise characteristics. Additionally, both of these SDRs have compatibility with GNU radio, which will be important for the signal processing side of the project. The biggest difference between these two SDRs is the signal processing capabilities which are much more capable with the B210 due to its integrated FPGA.

Amplifiers were also chosen based on their ability to perform within the hydrogen line bandwidth between 1400 - 1427 MHz. Both the Mini Circuit and SAWbird amplifiers perform well within this range, with the Mini Circuit amplifier having smaller noise figures than the SAWbird. The price and noise difference will allow us to compare price to noise to find how much signal loss it attributed to price.

Finally, the antenna materials are an estimate based on anticipated antenna size and the cost of plywood and aluminum sheeting.

Item	Part Name/Number	Cost
SDR	USRP B210 + Steel Enclosure	\$1674
SDR	RTL SDR Blog V3	\$27.75
Amplifier	SAWbird+ H1	\$45
Amplifier	Mini Circuit ZX60-33LN+	\$240
Antenna Materials	plywood, aluminum sheeting	\$250
		Total: \$2236.75

Table 2: Equipment list and overall budget for the project.

A.2 Senior Design Conference Slides



SANTA CLARA UNIVERSITY

School of Engineering

Cost Efficient Radio Telescope

Nick Arroyo, Brian Benedicto, Tyler Ikehara

Advisors: Dr. Kurt Schab, Dr. Shoba Krishnan

Department of Electrical and Computer

Engineering



Presentation Outline

- Motivation, Needs, and Objectives
- Background Information
- Project Design and Outcomes
- Summary and Concluding Thoughts



[1]https://upload.wikimedia.org/wikipedia/commons/0/00/CSIRO_ScienceImage_4350_CSIROs_Parkes_Radio_Telescope_with_moon_in_the_background.jpg

Motivation and Needs

- Radio Astronomy is a method to track the movements of celestial bodies in the observable universe
- Professional radio telescopes are massive and expensive
- Can we make a more accessible alternative?



FAST radio telescope located in southwest China. Is the one of largest single aperture telescopes in the world. The dish itself has a diameter of 500 meters.

Citizen Science

- Accelerate innovation through public participation
- Crowdsourcing scientific measurements
 - **City Nature Challenge** - An international effort for people to find and document plants and wildlife in cities across the globe
- More points of data acquisition

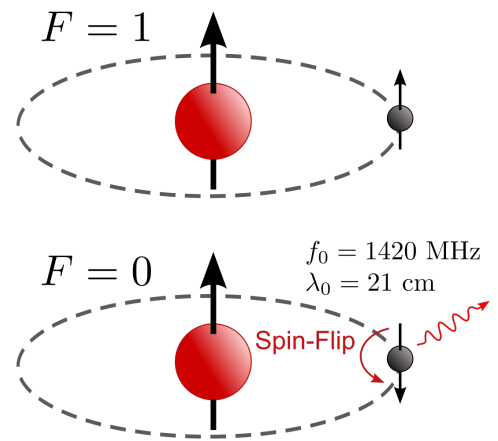


Objectives

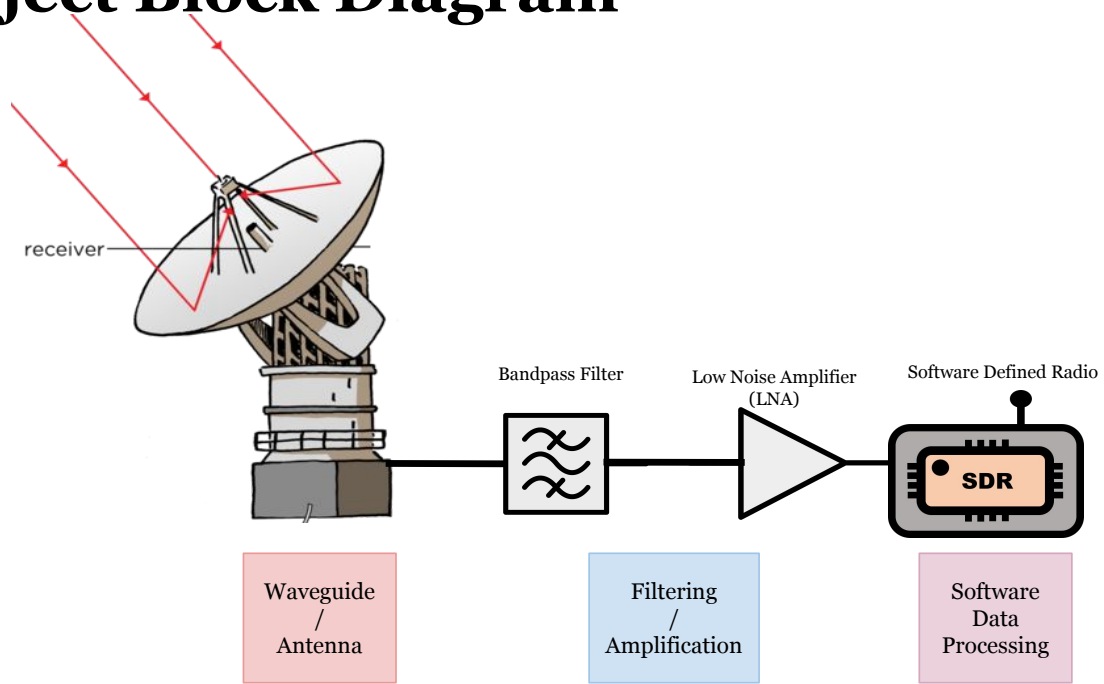
- To bring radio astronomy capabilities to Santa Clara University
- To design and build a cost efficient radio telescope
 - Select components to improve the performance of our system
 - Determine a way to locate observable bodies in space
- To create a proof-of-concept prototype that future teams at SCU can build upon

Background Information

- Large masses in the universe (planets, stars, galaxies) contain vast amounts of hydrogen
- Hydrogen radiates signals at a frequency of 1420 MHz due to electron spin-flips
- These signals can be observed and used to locate and map celestial bodies using a radio telescope



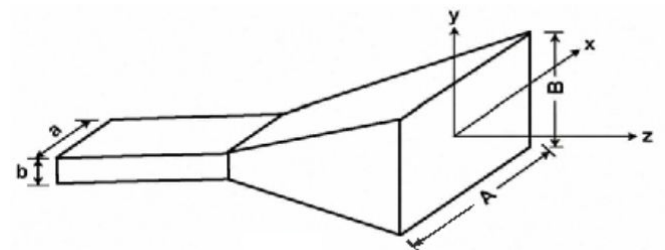
Project Block Diagram



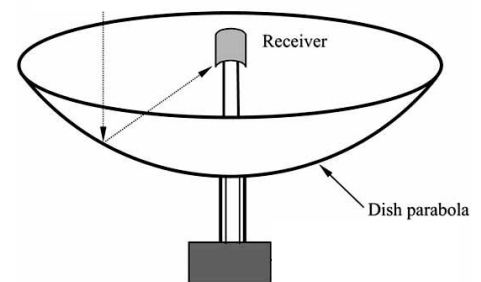
[5] <https://www.sivavula.com/read/science/grade-8/looking-into-space/16-looking-into-space?id=toc-id-2>
[6] <https://www.onesdr.com/2019/10/03/what-is-software-defined-radio-sdr/>

Antenna Design

- High directivity and gain
- Ease of construction
- Pyramidal horn antenna vs. parabolic dish antenna
 - Horn shields sidelobe noise
 - Dish requires a specific waveguide



Waveguide
/
Antenna



[7] https://www.researchgate.net/figure/fig-8-Schematic-diagram-of-a-parabolic-dish-collector_fig6_228343933
[8] Rong, Qiuyuan, and Donglin, 2010

Horn Antenna Design

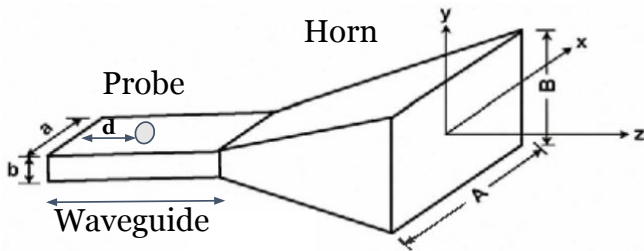


Table 1. Horn/Waveguide Dimensions

Waveguide Dimensions WR650 Standard	Horn Dimensions
$a = 0.165$ m	$A = 0.75$ m
$b = 0.083$ m	$B = 0.58$ m

$$1.) \quad A^4 - aA^3 + \frac{3bG\lambda^2}{8\pi\epsilon_{ap}}A = \frac{3G^2\lambda^4}{32\pi^2\epsilon_{ap}^2}$$

$$2.) \quad G = 0.51 \frac{4\pi}{\lambda^2} AB = 18 \text{ dB}$$

$G = 18$ dB is the gain of the antenna

$\lambda = 21$ cm is the wavelength at the design frequency

$f = 1420$ MHz

$\epsilon_{ap} = 0.51$ is the aperture efficiency

$$3.) \quad \lambda_g = \frac{\lambda}{\sqrt{1 - (f_c/f)^2}} = 28 \text{ cm}$$

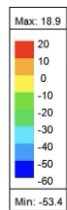
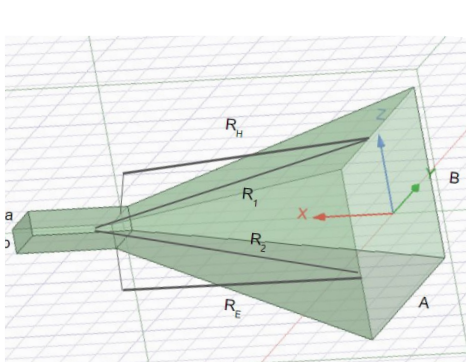
$$4.) \quad d = 0.25\lambda_g = 7 \text{ cm}$$

λ_g is the waveguide propagation wavelength

f_c is the cutoff frequency

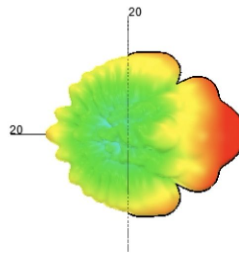
Horn Antenna Simulation (HFSS)

Waveguide
/
Antenna



Gain Plot 1

ANSYS



- Using the dimensions calculated in the previous slide
- Simulation results show a gain of **18.9 dB**
- Probe distance of $d = 0.4$ cm showed the best performance in HFSS

Horn Antenna Set-up and Testing



Arbitrary waveform generator +
RF signal generator



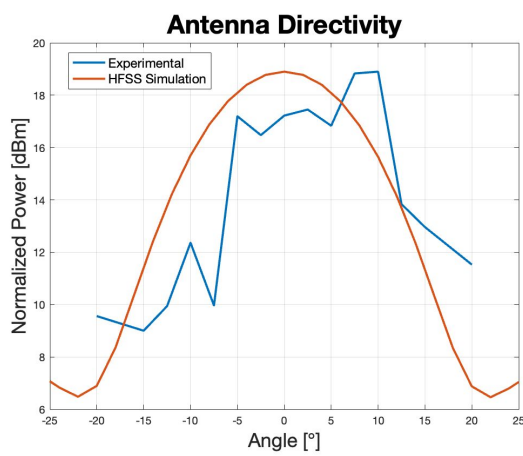
Over the air testing



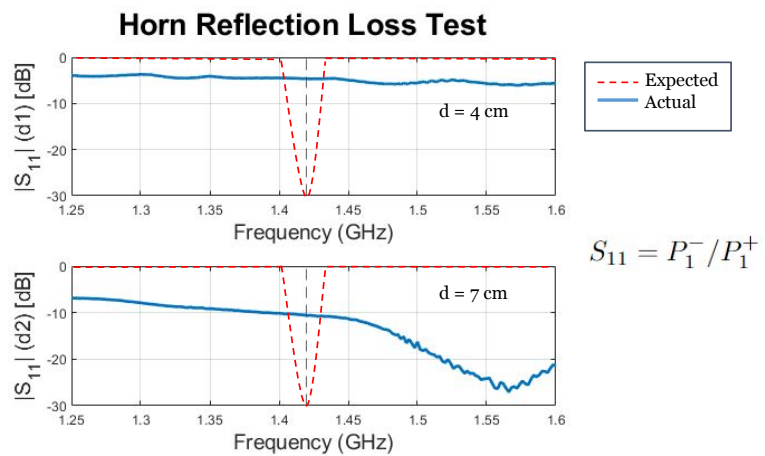
Coaxial feed to LNA input to
Field Fox spectrum analyzer

Horn Antenna Performance

Waveguide
/
Antenna



Over the air gain testing aligns with the simulated results

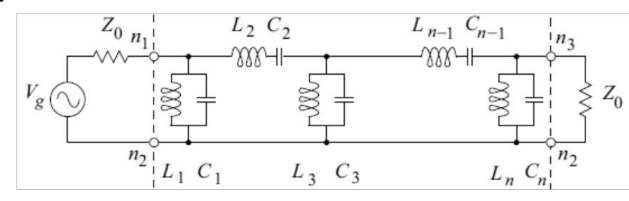
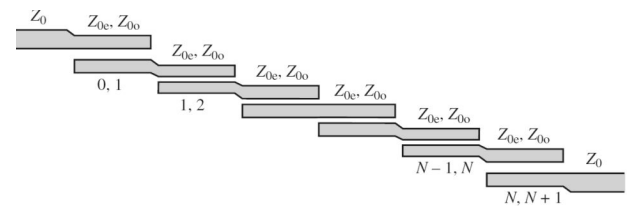


Comparison between different probe placement distances. Match at 1.55 GHz?

Bandpass Filter Design

Filtering / Amplification

- A Bandpass Filter to reject signals outside of our target bandwidth
 - 1400 MHz < freq < 1427 MHz
 - FCC allocated radio astronomy band
- Two candidate topologies
 - Lumped Element vs Coupled Line

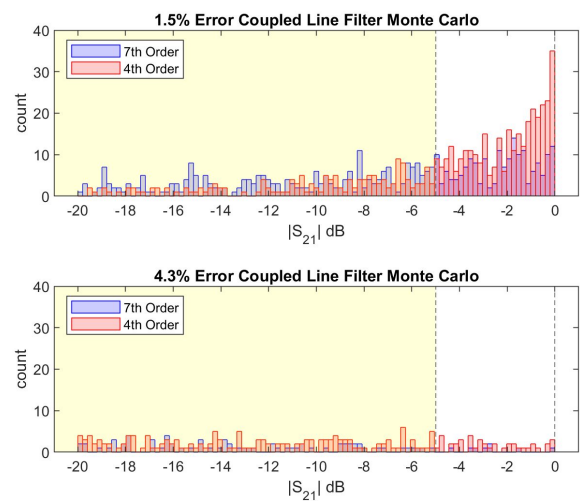


[10] https://www.google.com/search?q=coupled+line+filter&rlz=1C1AWFC_enUS816US816&source=lnms&tbn=isch&sa=X&ved=2ahUKEwiFopnQwNr3AhWiGTQIHf3sAH8Q_AUoAXoECAEQAw&biw=1536&bih=745&dpr=2.5#imgrc=SKJ_BopMMJxMdM
 [11] https://www.google.com/search?q=lumped+filter&rlz=1C1AWFC_enUS816US816&source=lnms&tbn=isch&sa=X&ved=2ahUKEwi18s7nwNr3AhWpCDQIHXPZBG4Q_AUoAXoECAEQAw&biw=1536&bih=745&dpr=2.5#imgrc=A4CrR7iB17wy-M

Coupled Line Bandpass Filter Design

Filtering
/
Amplification

- Monte Carlo simulation to verify design robustness
 - Adds specified level of error to dimensions (Gaussian)
- 4th order vs 7th order filter

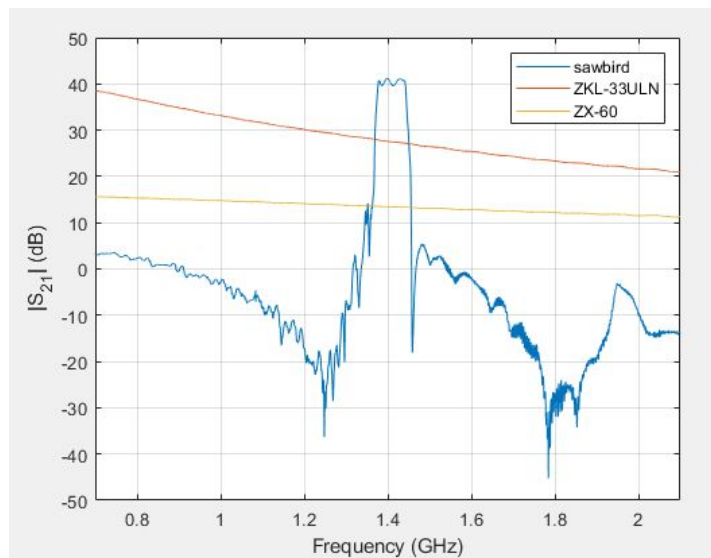


Low Noise Amplifier Gain Comparisons

- Searching for very low power signals requires high gain
- General purpose vs. special purpose LNAs

Table 2. Amplifier Gain Comparisons

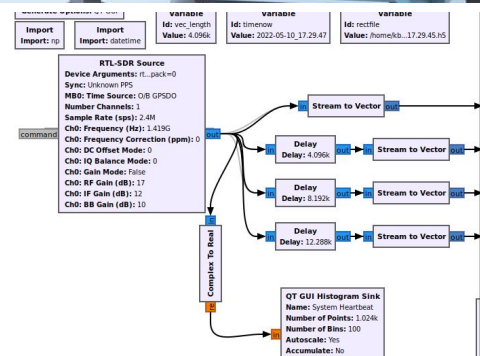
Amplifier	Gain at 1420 MHz
Sawbird	~40 dB
ZKL-33ULN	~28 dB
ZX-60	~14 dB



Full Spectrum Amplifier Response

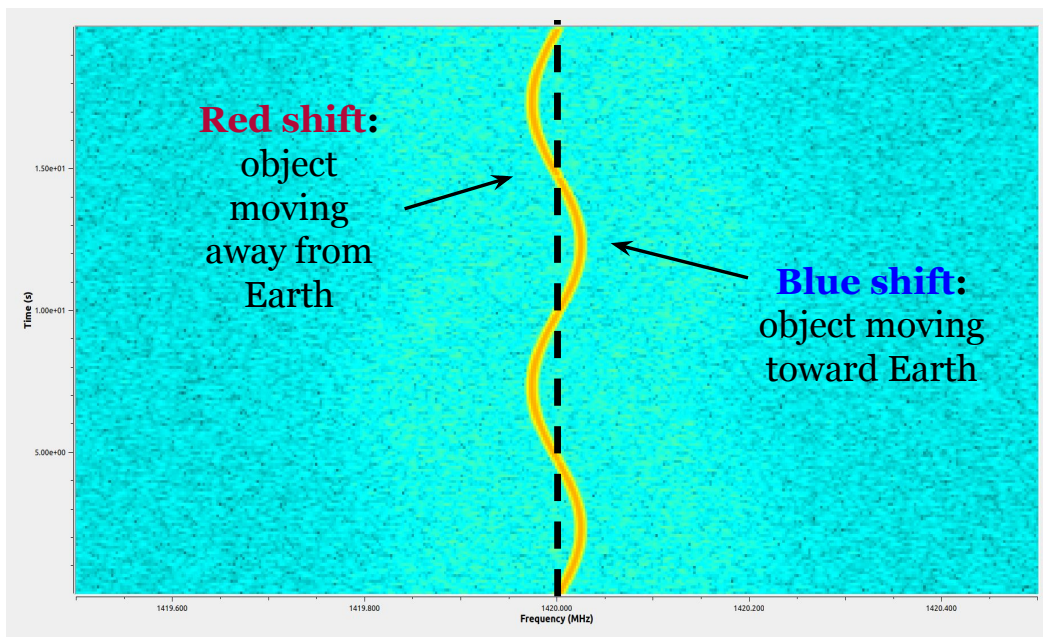
Software Defined Radios (SDR)

- Experimental receivers are expensive or made inhouse
 - Combination of many different pieces and bench equipment
- SDRs are a complete package
 - Provides a cost efficient method for processing radio frequencies.
 - Easy adaptations through software



[12] <https://www.icomamerica.com/en/products/amateur/receivers/r9500/specifications.aspx>

Waterfall Plots



SDRs for Radio Astronomy

- Few affordable radios for radio astronomy
- Adaptable performance and parameters for small hydrogen signals
- Developed software can easily be remodified to work on other SDRs.

	RTL SDR-Blog V3	Ettus B210
Application	hobbyist	industry
Noise floor	-78 dB	-100 dB
Computing	host computer	on-board FPGA
Cost	\$28	\$1674

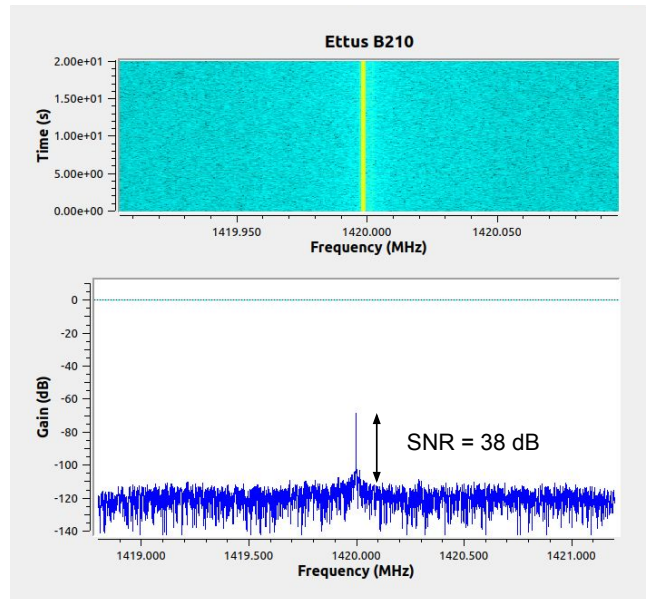
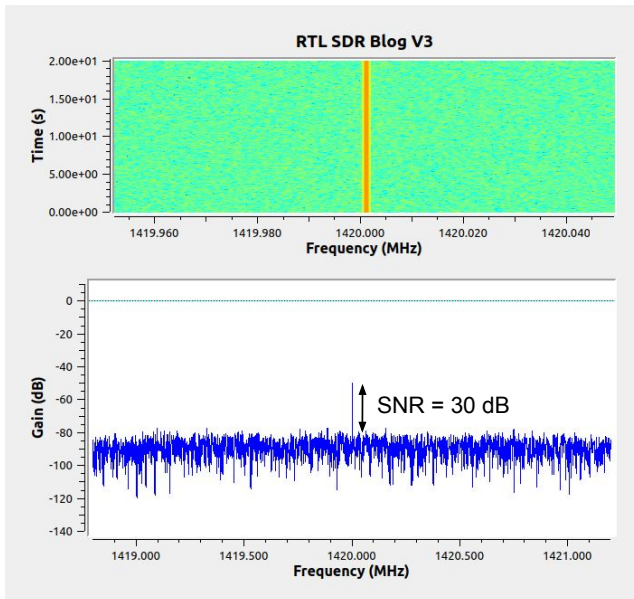


[13] <https://www.rtl-sdr.com/wp-content/uploads/2018/02/RTL-SDR-Blog-V3-Datasheet.pdf>

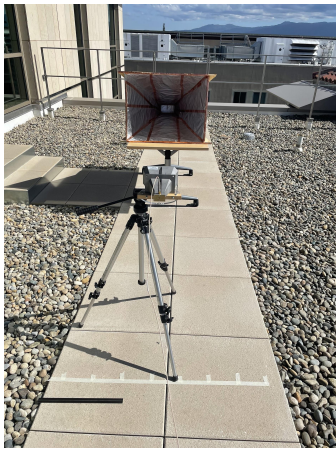
[14] <https://www.ettus.com/all-products/ub210-kit/>

SDR Comparisons

Software
Data
Processing



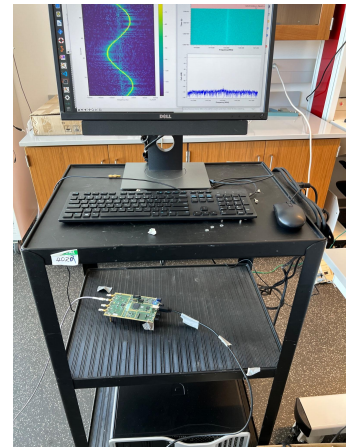
Complete Set-up and Testing



1420 MHz 67dBm w/ modulation
at 15 mHz, 700mV over the air

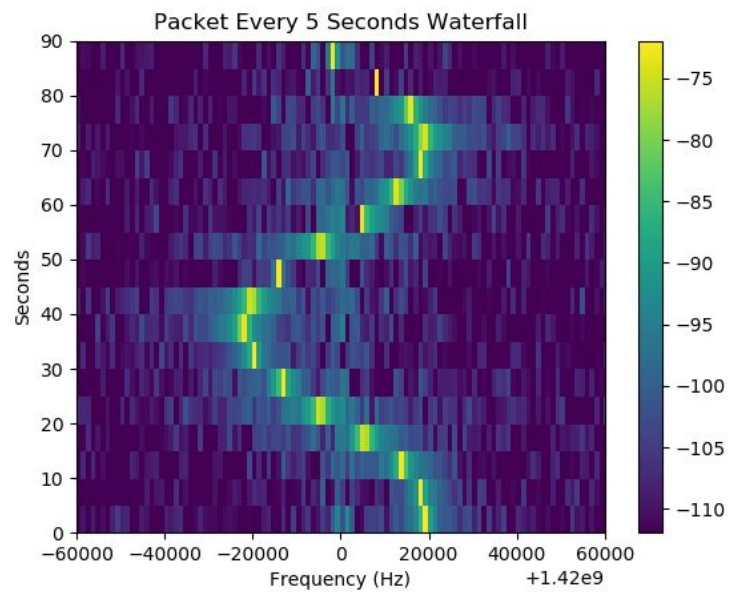
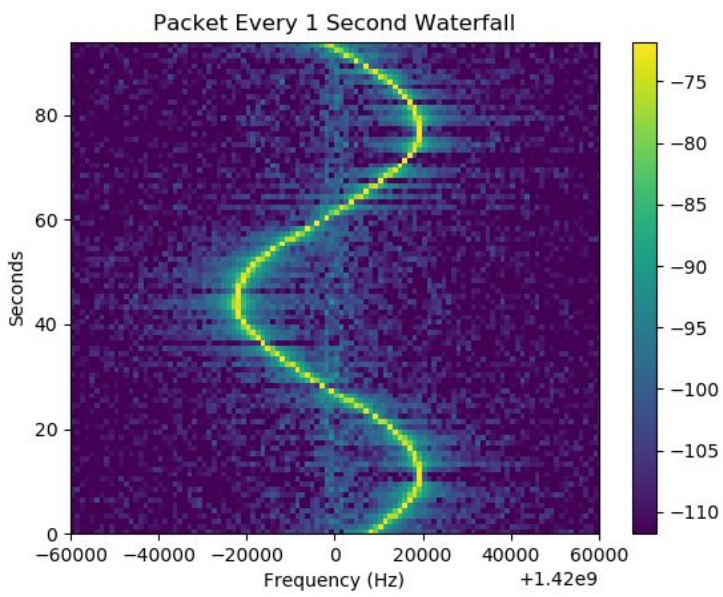


Coaxial feed to LNA input



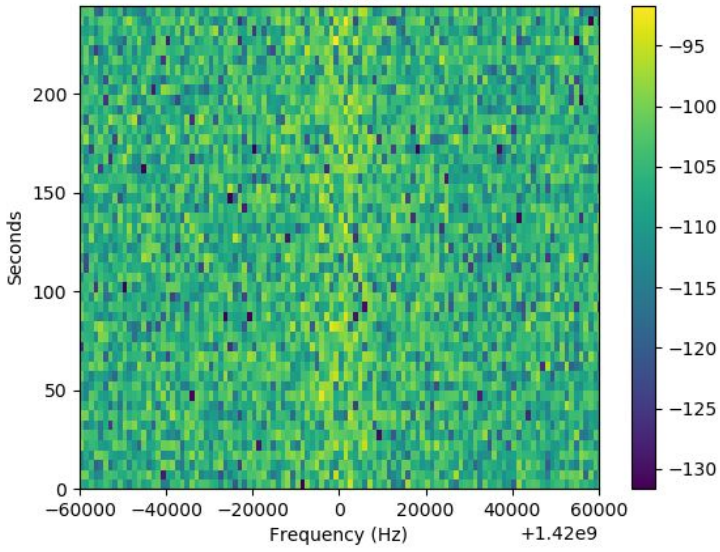
SDR receiving and processing

Final Tests

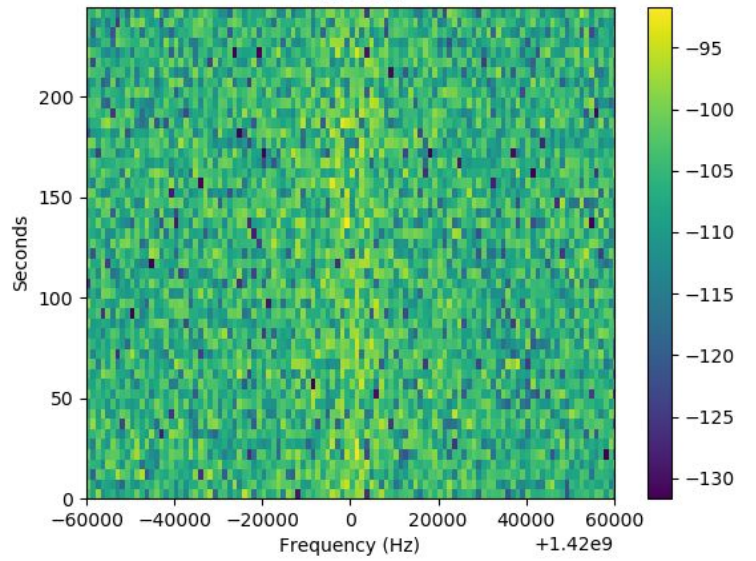


The Ultimate Test

No Sun



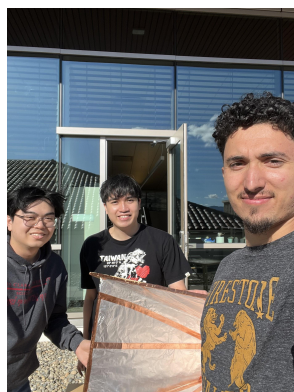
Sun Scan



Summary

- To bring Radio Astronomy capabilities to Santa Clara University ✓
- To design and build a cost efficient radio telescope ✓
 - Select and design filters and amplifiers to improve the performance of our system ✓
 - Create a script in order to determine the observable celestial bodies in our galaxy at any given time ✓
- To create a proof-of-concept prototype that future teams at SCU can build from ✓

Concluding Thoughts



We have created a successful proof of concept for Radio Astronomy at SCU!

The future of SCU Radio Astronomy?

[15]https://upload.wikimedia.org/wikipedia/commons/0/00/CSIRO_ScienceImage_4350_CSIROs_Parkes_Radio_Telescope_with_moon_in_the_background.jpg

Thank You!

Special thanks to our advisor Dr. Kurt Schab, Dr. Shoba Krishnan, The department of Electrical and Computer Engineering, and Xilinx.

References

1. https://upload.wikimedia.org/wikipedia/commons/0/00/CSIRO_ScienceImage_4350_CSIROs_Parkes_Radio_Telescope_with_moon_in_the_background.jpg
2. Wired.com: China built the world's largest telescope, <https://www.wired.com/story/china-fast-worlds-largest-telescope-tourists/>
3. <https://www.siyavula.com/read/science/grade-8/looking-into-space/16-looking-into-space?id=toc-id-2>
4. https://en.wikipedia.org/wiki/Hydrogen_line
5. <https://www.siyavula.com/read/science/grade-8/looking-into-space/16-looking-into-space?id=toc-id-2>
6. <https://www.onesdr.com/2019/10/03/what-is-software-defined-radio-sdr/>
7. https://www.researchgate.net/figure/fig8-Schematic-diagram-of-a-parabolic-dish-collector_fig6_228343933
8. K. Rong, L. Qiuyuan, and S. Donglin, "Analysis for phase center of pyramidal horn antennas for out of band," *Proceedings of the 9th International Symposium on Antennas, Propagation and EM Theory*, pp. 49-52, 2010.
9. W. L. Stutzman and G. A. Thiele, *Antenna Theory and Design*. Wiley, 2013.
10. LightWork Memo 29: Hydrogen Line Project Documentation https://docs.google.com/document/d/1_7ZOe1Et_8OTko7bgbTd7LLNqDAtgAimCS5oJM9JRbQ/edit
- 11.
12. <https://www.icomamerica.com/en/products/amateur/receivers/r9500/specifications.aspx>
13. <https://www.rtl-sdr.com/wp-content/uploads/2018/02/RTL-SDR-Blog-V3-Datasheet.pdf>
14. <https://www.ettus.com/all-products/ub210-kit/>
15. https://upload.wikimedia.org/wikipedia/commons/0/00/CSIRO_ScienceImage_4350_CSIROs_Parkes_Radio_Telescope_with_moon_in_the_background.jpg

A Compact Radio Telescope for the 21CM Neutral Hydrogen Line, Saje and Vidmar (p. 28), <http://antena.fe.uni-lj.si/literatura/Razno/Diplome/Radioteleskop/clanek/radioteleskop.pdf>

Daily image. Daily Image RSS. (n.d.). Retrieved November 12, 2021, from <https://www.astron.nl/dailyimage/main.php?date=20170511>.

<https://www.britannica.com/science/radio-telescope>